A ΛCDM Extension Explaining the Hubble Tension and the Spatial Curvature $\Omega_{k,0} = -0.012 \pm 0.010$ Measured by the Final PR4 of the Planck Mission

Horst Foidl[1,2*] and Tanja Rindler-Daller[1,2,3†]

[1] Institut für Astrophysik, Universitätssternwarte Wien, Fakultät für Geowissenschaften, Geographie und Astronomie, Universität Wien, Türkenschanzstr.17, A-1180 Vienna, Austria
[2] Vienna International School of Earth and Space Sciences, Universität Wien, Josef-Holaubek-Platz 2, A-1090 Vienna, Austria
[3] Wolfgang Pauli Institut, Oskar-Morgenstern-Platz 1, A-1090 Vienna, Austria

December 6, 2024

ABSTRACT

The measurements of the CMB have determined the cosmological parameters with high accuracy, and the observation of the flatness of space have contributed to the status of the concordance ΛCDM model. However, the cosmological constant Λ, necessary to close the model to critical density, remains an open conundrum. We explore the observed late-time accelerated expansion of the Universe, where we consider that the Friedmann equation describes the expansion history of FLRW universes in the local reference frame of freely falling comoving observers, which perceive flat, homogeneous and isotropic space in their local inertial system, where, as a consequence of the equivalence principle, special relativity applies. We use this fact to propose an extension to ΛCDM, incorporating the initial conditions of the background universe, comprising the initial energy densities as well as the initial post big bang expansion rate. The observed late-time accelerated expansion is then attributed to a kinematic effect akin to a dark energy component. Choosing the same $\Omega_{m,0} \simeq 0.3$ as ΛCDM, its equation of state $w_{de} \simeq -0.8$. Furthermore, we include the impact on the expansion history caused by the cosmic web of the late Universe, once voids dominate its volume, and find that the initially constant w_{de} becomes time-dependent, evolving to a value of $w_{de} \simeq -0.9$ at the present. While this impact by voids is minor, it is sufficient to provide a solution to the Hubble tension problem. We use CLASS to calculate the expansion history and power spectra of our extension and compare our results to concordance ΛCDM and to observations. We find that our model agrees well with current data, in particular with the final data release PR4 of the Planck mission, where it explains the reported spatial curvature of $\Omega_{k,0} = -0.012 \pm 0.010$.

1. Introduction

The nature of the cosmological constant Λ has been a challenging open problem in modern cosmology. The issue has intensified over the years, as the current concordance model of ΛCDM – with cold dark matter (CDM) the other open conundrum –, continues to pass many observational tests, especially on the large scales of the cosmic web, or the cosmic microwave background (CMB) radiation. In particular, the CMB measurements have invigorated the flat universe interpretation, i.e. that the space of the background universe has no curvature.

However, it was reasoned that the amount of baryonic matter predicted by big bang nucleosynthesis was far too small to explain a flat universe (e.g., Steigman (2007)), and even the addition of a substantial amount of dark matter (DM) in the form of CDM, whose presence was not in doubt any longer by the late 1980s, was not sufficient to get a universe at critical density, in order to get a flat geometry of space. In fact, age determinations of the oldest known stars ruled out the Einstein-de Sitter (EdS) model as a viable model, which could have otherwise been a model for a CDM-dominated universe at the present, with its critical density provided by matter only (see e.g. Weinberg (2008)). Finally, in accordance with the predictions from inflation (Guth (1981)), the observations of the CMB by the balloon-based BOOMERanG experiment (de Bernardis et al. (2000)

and MacTavish et al. (2006))), as well as observations with increasing accuracy by the space missions COBE (Smoot et al. (1992)), WMAP (Hinshaw et al. (2013)) and Planck (Planck-Collaboration (2020)), boosted the flat universe interpretation. This, and the previous discovery of the accelerated expansion of the Universe (Perlmutter et al. (1999); Schmidt et al. (1998); Riess et al. (1998); Perlmutter (2003)), led to the empirical addition of the cosmological constant Λ, in order to get a universe at critical density, that is a *flat universe* and the ΛCDM concordance model became the standard model of cosmology.

Despite the great success of ΛCDM, the still unknown nature of CDM and the nature of the cosmological constant Λ, which, according to measurements, each contribute roughly 25% and 70%, respectively, to the present-day energy density of the Universe, remain pending questions. Many cosmological observation campaigns analyze their data, not only in light of testing ΛCDM, but also to examine possible extensions to ΛCDM, which replace the cosmological constant Λ with different alternative models of dark energy (DE), which employ a time-dependent equation of state (EoS) parameter $w = p/\rho$ (The energy density ρ and the pressure p are commonly understood as components of some physically or operationally defined DE component).

Prominent examples of campaigns include the Dark Energy Survey, see for example, the Year 3 (DES-Y3) results in Abbott et al. (2022, 2023), or the CMB measurements by Planck-Collaboration (2020). They use the so-called "CPL parametriza-

* horst.foidl@outlook.com
† tanja.rindler-daller@univie.ac.at

tion" by Chevallier & Polarski (2001); Linder (2003) for the EoS parameter,

$$w(a) = w_0 + (1 - a) w_a, \tag{1}$$

which is defined for $a \in [0, 1]$, where a is the scale factor[1]. The CPL parametrization is simple and empirically defined, with no physical motivation for the evolution of $w(a)$ being linear in a. In Foidl & Rindler-Daller (2024) we exemplify, based on empirical arguments, that a cosmological model including a CPL-based DE component with an EoS parameter w_{de} evolving from -0.8 to -0.9 describes the CMB temperature spectrum of ΛCDM and yields a Hubble constant H_0 being compatible with direct measurements (e.g., Riess et al. (2022)) in the local Universe. In contrast, however, in this paper we propose physically motivated extensions to ΛCDM – wCDM and owCDM – with a time-dependent EoS parameter w_{de} of its effective DE component also evolving from -0.8 to -0.9, which we would like to put up for discussion[2].

In the first part of this paper, we reassess ΛCDM's flat universe interpretation, where we consider that the Friedmann equation describes the expansion history of Friedmann-Lemaître-Robertson-Walker (FLRW) universes in the local reference frame of comoving observers, which perceive flat, homogeneous and isotropic space in their local inertial system, based on the equivalence principle (see e.g., Weinberg (1972, 2008), Peacock (1999) or Fließbach (2016)). Thus, the measurements of the CMB, reporting the flatness of space, confirm that we fulfill the criterion of a comoving observer to a high degree. We interpret the expansion history of the background universe as an initial value problem (IVP), where the post big bang initial conditions (ICs) in the early Universe are given by the initial densities of the cosmic components in the Universe (radiation, baryons and DM) and the post big bang expansion rate H_{ini}.

In the second part of this paper, we find that the kinematic effects induced by the initial expansion rate (post big bang) and the initial density of the background universe, can be described in a straightforward manner by associating the operationally defined quantity ρ_{de}, dark energy, replacing ρ_Λ, with an EoS, being different from that of a cosmological constant. Choosing for the other parameters the same values as for the ΛCDM concordance model, our wCDM model yields $w_{de} \sim -0.8$, which results in an expansion history very close to ΛCDM with its $w_\Lambda = -1$.

In the third part of the paper, we include in our ΛCDM extension the effects of the cosmic voids, which dominate the volume of the Universe in the late stages of the evolution of the cosmic web. The resulting backreaction from voids also affects the evolution of the expansion rate. We consistently include this effect into ρ_{de}, using void models informed by cosmological ΛCDM simulations of the previous literature, and parameterize it by deriving the necessary modifications to the heretofore constant EoS parameter w_{de}, that becomes a function of time, or scale factor, respectively, once the voids dominate the volume of the Universe. In fact, the initial value of $w_{de}(a) \sim -0.8$ decreases to

---

[1] In practice, cosmological codes, including the one we use (CLASS), in the default configuration compute observables not earlier than at $a = 10^{-14}$.

[2] We use these acronyms for our models, as they are used frequently in the literature to express an extension to ΛCDM, particularly for dynamical models of DE, without and with spatial curvature, respectively (see e.g. Dark Energy Survey Year 3 Results Abbott et al. (2023), Planck-Collaboration (2020) and the Particle Data Group Review, Chapter 28 "Dark Energy" Particle Data Group et al. (2022)).

$w_{de}(1) \sim -0.9$ at the present where the scale factor $a = 1$. Thus, it gets closer to the EoS of a cosmological constant. As a result, the present-day value of the expansion rate H_0, i.e. the Hubble constant, shifts to a higher value, compared to the value it would have, if the EoS parameter remained constant throughout cosmic time (see also Foidl & Rindler-Daller (2024)). Although the expansion rate is changed by only about 8% due to the impact of voids, it is enough to provide a solution to the Hubble tension problem.

By comparing our results with cosmological observations, we find that our ΛCDM extension is in agreement with current data. To this end, we apply our proposed procedure by Foidl & Rindler-Daller (2024) to our model and fit it to the ΛCDM CMB spectrum and $H_0 = 73.04$ km/s/Mpc as determined by Riess et al. (2022) in the local Universe, where we, in addition to wCDM, consider also spatial curvature. The resulting owCDM model perfectly agrees with the final results of the Planck mission (Tristram et al. (2024)), in particular with the reported spatial curvature of $\Omega_{k,0} = -0.012 \pm 0.010$.

This paper is organized as follows. In Sec. 2 we recapitulate the basic equations for the evolution of the background universe in FLRW models. Sec 3 investigates the flat universe interpretation for the general case of FLRW universes, followed by a discussion of the ICs of the background universe. Sec. 4 proposes a ΛCDM extension, such that the cosmological model incorporates the post big bang initial conditions of the early Universe. Sec. 5 contains our treatment and derivation of the impact of cosmic voids onto the expansion history. This impact is minor, but significant enough that it provides a possible resolution to the Hubble tension problem. In the following Sec. 6, we present the results of the numerical simulations of our ΛCDM extension wCDM, based on our amended version of the code Cosmic Linear Anisotropy Solving System (CLASS), where we also compare our results with the concordance ΛCDM model, as well as with observations. In Sec. 7 we present the results of our owCDM model and compare it to Planck's PR4 (Tristram et al. (2024)). Finally, in Sec. 8, we summarize the presented concepts, results and implications, also in light of cosmological observations.

2. Basic Equations for the Expansion History in FLRW Models

First, we recapitulate the equations involved in the description of the evolution of the homogeneous and isotropic background universe, we need in the following. As gravity is the only force acting on cosmological length scales, it determines the evolution of the background universe and is described by Einsteins' field equations

$$R_{\mu\nu} - \frac{1}{2} g_{\mu\nu} R = \frac{8\pi G}{c^4} T_{\mu\nu}, \tag{2}$$

with the Ricci tensor $R_{\mu\nu}$ and the Ricci scalar R. The left-hand side (lhs) of the equation is often expressed as $E_{\mu\nu}$, the Einstein tensor. The right-hand side (rhs) contains the energy-momentum tensor $T_{\mu\nu}$, which includes the cosmic inventory of given cosmological models. The energy-momentum tensor $T_{\mu\nu}$ determines the curvature of space, expressed by the metric $g_{\mu\nu}$, which is also included in the Ricci tensor $R_{\mu\nu}$ and the Ricci scalar R. Cosmological models differ in their assumptions on the nature and amount of the cosmic components encoded in $T_{\mu\nu}$. As such, all models are subject to observational constraints.

The geometry of a universe with constant curvature is described by applying the Riemannian formalism of curved surfaces and was developed by Robertson (1936b) and Walker (1937) based on Milne's idea of a kinematically determined universe (Milne (1933)) and preceding works by Friedmann Friedmann (1922, 1924) and Lemaître (1927). In spherical coordinates (r, θ, ϕ), the line element of the metric reads as

$$ds^2 = c^2 dt^2 - R^2(t)\left(\frac{dr^2}{1 - kr^2} + r^2 d\Omega^2\right) \tag{3a}$$

$$d\Omega^2 = d\theta^2 + \sin^2\theta d\phi^2, \tag{3b}$$

with k the curvature index and its values $+1$ (closed universe), 0 (flat universe), -1 (open universe). The spatial coordinates (r, θ, ϕ) are defined in the comoving frame where r, θ and ϕ remain "fixed", corresponding to the assumption of spaces of constant global curvature (the geometry of the Universe). $R(t)$ is the "radius of curvature", as called by Kolb & Turner (1990), at cosmic time t (for $k = \pm 1$), with the dimension of length.

Applying the FLRW metric (3) to the metric tensor $g_{\mu\nu}$ in the Einstein equations (2), the energy-momentum tensor $T_{\mu\nu}$ then takes a perfect-fluid form, which reads

$$T^{\mu\nu} = \left(\rho + \frac{p}{c^2}\right)u^\mu u^\nu - g^{\mu\nu} p. \tag{4}$$

with u^μ and u^ν the four velocities $\gamma(c, \boldsymbol{u})$ and $\gamma = 1/\sqrt{1 - u^2/c^2}$. The time-time component of the solution to the Einstein equations (2) yields the (first) Friedmann equation in the *classical version*, as derived by Friedmann (1922), see for example Kolb & Turner (1990),

$$H^2(t) = \frac{8\pi G}{3c^2}\rho - \frac{kc^2}{a^2(t)}, \tag{5}$$

which describes the dynamics of the evolution of the background universe. Here, ρ refers to the entire energy density of the Universe; k is the curvature index, defined in Eq. (3) determining the geometry, as $k = +1$ for a closed (supercritical, density greater than the critical density) universe, $k = -1$ for an open (subcritical, density less than the critical density) universe and $k = 0$ for a flat geometry with critical density. In the forthcoming we use the notion "geometry" for the curvature of the Universe as determined by the FLRW metric (3) and the Friedmann equation (5), respectively. a refers to the scale factor, with the dimension of length, which, owing to the symmetries imposed by the isotropy and homogeneity of the background universe, is a function of cosmic time t and is defined as the relative "size" of an expanding or contracting universe, relative to its present-day size $|a_0| = 1$. H is the Hubble parameter (we use the term expansion rate interchangeably) defined as

$$H(t) = \frac{\dot{a}}{a}, \tag{6}$$

where the dot refers to the derivative with respect to cosmic time t. The space-space component yields the second Friedmann equation

$$\frac{\ddot{a}}{a} = -\frac{4\pi G}{3c^2}(\rho + 3p), \tag{7}$$

which Friedmann called the deceleration equation. In recent literature it is called the acceleration equation.

Now, let us introduce the cosmic inventory which features the current concordance ΛCDM model. Also, we introduce some standard notions and equations which we need in the paper. The energy densities of interest include cold dark matter ("CDM"), baryons ("b") and radiation ("r") (including photons and neutrinos). In the formulae, we also include the cosmological constant Λ, empirically added to the cosmic inventory to explain the flatness of space.

In order to study a variety of cosmological models, it has become customary to put "curvature" as well as the cosmological constant "Λ" into the energy-momentum tensor $T_{\mu\nu}$, by operationally defining "effective" energy densities for them, namely $\rho_k = -3kc^2/(8\pi G a^2)$ for curvature ("k"), and $\rho_\Lambda = \Lambda c^2/(8\pi G)$ for the cosmological constant. In the ΛCDM model, $\rho_k = 0$ is prescribed, while $\rho_\Lambda \neq 0$, such that Λ closes the Universe to critical density (see Eq. (15)).

We stress that, although ρ_k represents a geometric quantity, it has morphed into a "substance," or cosmic inventory, described by $T_{\mu\nu}$, upon this standard operational procedure. Nevertheless, it is rightfully not regarded a physical constituent of the Universe, but simply a mathematical formalism, contributing an effective or artificial contribution to $T_{\mu\nu}$. On the other hand, Λ is usually regarded as a real physical cosmic inventory in ΛCDM, which contributes to $T_{\mu\nu}$ basically in the same manner as matter and radiation.

The Friedmann equation in *modern* language reads as

$$H^2(t) = \frac{8\pi G}{3c^2}\left[\rho_r(t) + \rho_b(t) + \rho_{\text{CDM}}(t) + \rho_k(t) + \rho_\Lambda(t)\right], \tag{8}$$

with the time-dependent background energy densities for radiation (ρ_r), baryons (ρ_b), CDM (ρ_{CDM}), the curvature (ρ_k), as well as the cosmological constant (ρ_Λ). $H(t)$ is the Hubble parameter and its present-day value[3], the Hubble constant, is denoted as H_0. The critical density, defining a flat universe, is given by

$$\rho_{\text{crit},t} = \frac{3H^2(t)c^2}{8\pi G}, \tag{9}$$

derived from (5) with vanishing curvature term. It is convenient to introduce the so-called density parameters or cosmological parameters

$$\Omega_{t,i} = \frac{\rho_i(t)}{\rho_{\text{crit},t}}, \tag{10}$$

where $i = $ CDM, b, r, etc., and which are nothing but the background energy densities relative to the critical density (9).

In order to solve the Friedmann equation, customarily, the energy conservation equation is applied (for each component $i = $ CDM, b, r,...), which reads

$$\frac{\partial \rho_i}{\partial t} + 3H(\rho_i + p_i) = 0, \tag{11}$$

where ρ_i and p_i stand for the respective background energy densities and pressures[4]. The energy densities and pressures are each related by their respective EoS,

$$p_i(t) = w_i(t)\rho_i(t), \tag{12}$$

---

[3]The literature has adopted the notational subscript "0" to denote present-day values, not the values at $t = 0$.

[4]This equation assumes that there is no transformation between different components.

where w_i is often called the EoS parameter, which can also change with time, in general. However, in ΛCDM, w_i is assumed to be a constant[5] for every component i =CDM, b, r, Λ and k. Assuming a constant EoS parameter w_i and using (12) in (11), it follows that $\dot{\rho}_i/\rho_i = -3(1+w_i)\dot{a}/a$, which is readily integrated to yield the well-known relation

$$\rho_i(a) = \Omega_{i,0}\rho_{\text{crit},0} \, a^{-3(1+w_i)}, \tag{13}$$

which describes the evolution of the background energy densities as a function of the scale factor a for constant w_i. The background evolution of the standard cosmic components is thus given by

$$\rho_r(a) = \Omega_{r,0}\rho_{\text{crit},0}/a^4 \tag{14a}$$

$$\rho_m(a) = \Omega_{m,0}\rho_{\text{crit},0}/a^3 \tag{14b}$$

$$\rho_k(a) = \Omega_{k,0}\rho_{\text{crit},0}/a^2 \tag{14c}$$

$$\rho_\Lambda = \Omega_{\Lambda,0}\rho_{\text{crit},0}, \tag{14d}$$

with (14a) for radiation (its EoS parameter in (12) is $w_r = 1/3$); (14b) for baryonic matter and for CDM ($w_m = 0$); (14c) for curvature ($w_k = -1/3$), and (14d) for the cosmological constant Λ ($w_\Lambda = -1$).

The Friedmann equation can be alternatively written as an algebraic closure condition. At the present, it reads

$$1 = \Omega_{r,0} + \Omega_{b,0} + \Omega_{\text{CDM},0} + \Omega_{k,0} + \Omega_{\Lambda,0}. \tag{15}$$

In other words, Eq. (15) is the normalization of the Friedmann equation (8) to the critical density.

3. The Flat Universe Interpretation

The ΛCDM model is a member of the broader family of FLRW cosmological models. Furthermore, a flat space in the Universe is assumed on the grounds of the curvature of space, as measured for example by the observations of the CMB – the flat universe interpretation, where the curvature term in the Friedmann equation (5) is customarily interpreted to express the geometry of the Universe. We will now reassess this interpretation.

3.1. Curvature in FLRW Universes

Let us elaborate on the curvature term appearing in the Friedmann equation (5), which is connected to the curvature factor in the FLRW metric (3). The derivation of Eq. (5), see for example Kolb & Turner (1990), suggests that the curvature term should not be confused with a contribution to the energy momentum tensor, which determines the Riemann tensor in the Einstein equations (2). It is these equations which ought to determine the global curvature of space in the Universe. We now reevaluate the interpretation of the curvature term of Eq. (5), in order to discuss whether it describes the global curvature of space or not, as follows.

In a first step, we use the Einstein equations (2) only, which describe the curvature of space, determined by the energy momentum tensor $T_{\mu\nu}$, that describes the distribution of energy (or matter) in the Universe. Presuming the cosmological principle,

$T_{\mu\nu}$ takes the form for a perfect fluid, given in Eq. (4), where the respective densities and pressures of the cosmic components of interest are considered. Applying $T_{\mu\nu}$ and solving the Einstein equations (2) yields the metric tensor $g_{\mu\nu}$, which describes the global curvature of space in the Universe. Considering, for example, the EdS universe, we apply $T_{\mu\nu}$ with the density at critical density and zero pressure for pressureless matter, which yields a non-flat metric tensor $g_{\mu\nu}$. This is easily seen in a kind of cross-check by solving the Friedmann equation for the EdS universe $H^2 = (8\pi G/3c^2)\rho_{\text{crit}}$, which yields $H^2(a) \propto a^{-3}$. Thus, we see a deceleration of the expansion rate H in the course of the expansion of the EdS universe, which is caused by gravity (see e.g., Peacock (1999)). It is important to note that no curvature term appears in Eq. (5) for the EdS universe.

In a second step, we follow the steps of the derivation of the Friedmann equation (5), described in Sec. 2 and reverse the procedure of step one. In contrast to the procedure of step one, determining the curvature of space for a given $T_{\mu\nu}$, we start by specifying the metric tensor $g_{\mu\nu}$ corresponding to the curvature term of Eq. (5). Applying this metric tensor $g_{\mu\nu}$ to the Einstein equations (2) yields $T_{\mu\nu}$ of the corresponding energy densities[6]. The obtained energy momentum tensor(s) is(are) checked for agreement with the one we used in the first step. We continue with the example of the EdS universe: the curvature term in (5) vanishes for the EdS universe and the corresponding metric tensor $g_{\mu\nu}$ describes flat space, which yields the energy momentum tensor $T_{\mu\nu}$ of empty space. This is different from a space at critical density in the EdS universe. Thus, in general, the curvature term does not express the spatial curvature[7]. This is addressed by Robertson (1936a), by using an "auxiliary" (mathematical) space associated with the FLRW metric (3) (based on Riemannian geometry), which categorizes the dynamics of expansion of the background universe via the curvature index $k \in \{-1, +1, 0\}$ as open (negative curvature), closed (positive curvature) and flat (no curvature), based on the energy density of the background universe relative to the critical density[8]. Walker (1937) uses the term "Riemannian space" for the space connected to the metric.

However, with regard to ΛCDM, the question arises as to how it is possible that observations of the CMB report the flatness of space given that the Universe is not empty, which we discuss as follows. The Friedmann equation (5) describes the dynamics of the expansion of the background universe, expressed by the evolution of the expansion rate $H(t)$ in the local reference frame of observers comoving with the expansion, moving on geodesics, that is freely falling FLRW observers[9]. The expansion rate $H(t)$ is determined by the two contributing terms describing the evolution of the density and the curvature, determined by Eqs. (14). A consequence of the equivalence principle of general relativity (GR) is that observers, freely falling in a gravitational potential, reside in a local inertial system, where special relativity (SR) ap-

---

[5]However, for a detailed study of phase transitions in the early Universe, it is important to include e.g. a variable EoS of the radiation component, in order to take into account the reduction of relativistic degrees of freedom in the wake of the Universe's expansion.

[6]In general, this solution is not unique.

[7]To falsify the assumption that the curvature term in Eq. (5) expresses the curvature of space, one contradicting example is sufficient.

[8]The definition of k refers to the density although the density does not appear in the metric. In the FLRW formalism this is addressed by the normalized Friedmann equation (15), relating density and curvature. Consequently, in the FLRW formalism, the density parameters of subcritical and supercritical universes are also normalized to critical density, for example by considering the suitable amount of curvature. Remember, the curvature is not regarded as a physical contribution to the energy budget of the Universe.

[9]The comoving observer is called fundamental observer by Robertson (1935). This term is also sometimes used in the literature.

plies, that is, they perceive flat space (see e.g., Weinberg (1972, 2008), Peacock (1999) or Fließbach (2016)). Moreover, a consequence of this is, that space appearing flat to comoving FLRW observers is irrespective of the energy density of the model universe. Thus, space appears flat to comoving observers in open, closed and flat universes, justifying $\rho_k = 0$ and $\Omega_{k,0} = 0$ in the ΛCDM model and provides the reason for the observation of the flatness of space, not necessarily connected to the critical density. This again suggests that the curvature term in the Friedmann equation Eqs. (5) and (8) does not express the global spatial curvature, as determined by the Einstein equations (2).

Therefore, the interpretation of the curvature term in Eq. (5) is still a pending question, as the term is not related to ρ_k and $\Omega_{k,0}$, respectively, which express the observed flatness of space, by us as free-falling FLRW observers[10].

3.2. The Initial Conditions of FLRW Universes

Customarily, the geometry (open, closed or flat) of a model universe is explained based on the energy density of the background universe relative to the critical density. We present a more general definition based on the ICs of the background universe, comprising of the initial densities in the early Universe, as well as the initial (post big bang) expansion rate.

The expansion rate for a universe at critical density is described by the Friedmann equation with vanishing curvature term

$$H^2 = \frac{8\pi G}{3c^2} \rho_{\text{crit}}, \tag{16}$$

This relation between expansion rate H and ρ_{crit} holds true for the entire cosmic time. In particular, also in the very first moments after the big bang. More precisely, the initial boost in the expansion rate is supposed to be provided immediately after the big bang. By the time we can apply GR, we can define an initial expansion rate H_{ini} (in the language of Lemaître, we could call it here "the primeval expansion rate"). As of this cosmic point in time, when we can meaningfully talk about the Friedmann equation, the Universe experienced its first deceleration phase (see e.g. Harrison (2000)), and the metric would appear flat for a comoving FLRW observer.

On the other hand, we can express the critical density for a flat universe by

$$\rho_{\text{crit}} = \frac{3H_{\text{ini}}^2 c^2}{8\pi G}, \tag{17}$$

which is simply Eq. (16) rearranged to express ρ_{crit} at the considered initial point in time. This defines the "critical expansion rate," for a given initial density as

$$H_{\text{crit}}^2 = \frac{8\pi G}{3c^2} \rho_{\text{ini}}. \tag{18}$$

We can interpret this relation as follows. Given an arbitrary initial energy density ρ_{ini} of a universe, originating from the big bang, the primeval expansion rate H_{ini} has to be specifically fine-tuned, in order to fulfill criterion (18) describing a universe with flat geometry, that is $H_{\text{ini}} = H_{\text{crit}}$.

---

[10]The fact that we are not perfect FLRW observers has ramifications, which we study in Section 7.

However, there are no comprehensible arguments, why the big bang should be restricted to this exclusive fine-tuned value for H_{ini}. In case H_{ini} is less than H_{crit} (or in other words, the ρ_{ini} is higher than ρ_{crit}, in order to fulfill Eq. (18)), the evolution of the universe is described by a closed geometry. An open geometry is determined by H_{ini} greater than H_{crit} (or ρ_{ini} being lower than ρ_{crit}, fulfilling Eq. (18)).

Limiting ourselves to a flat geometry and given the energy densities as deduced by the measurements of the CMB (e.g., by Planck-Collaboration (2020)) in ΛCDM, it thereby ignores from the outset a broad range of possible initial expansion rates H_{ini}. Hence, the assumption of a flat geometry in the FLRW metric does not cover those initial expansion rates H_{ini}, which would lead to subcritical and supercritical universes, where, as shown in Sec. 3.1, freely falling, comoving observers likewise perceive flat space.

4. A ΛCDM Extension to incorporate the Initial Conditions

In Sec. 3.1, we argue that a prospective observation of flat space does not necessarily imply a universe at critical density, since the curvature terms ρ_k and Ω_k in Eqs. (8) and (15), respectively, vanish in the local inertial frame of comoving FLRW observers, giving the reasons for the flatness of space as measured by the observations of the CMB. In order to interpret the curvature term in Eq. (5), we associate the general concept of DE with the geometry of the FLRW metric (3) and use the subscript "de" for the quantities describing the dynamics of expansion in the forthcoming.

In Sec. 3.2 we argue that the ICs of the background universe are given by the initial expansion rate H_{ini} and the initial densities. Based on the CMB measurements, within the ΛCDM model, the initial densities are determined to high precision (see also Foidl & Rindler-Daller (2024)). For this reason, it is sufficient to incorporate H_{ini} into the ΛCDM formalism. Let us proceed in our approach by considering the following parameters

$$1 = \Omega_{r,0} + \Omega_{b,0} + \Omega_{\text{CDM},0} + \Omega_{k,0} + \Omega_{\text{de},0}, \tag{19}$$

where the operationally defined density parameter of the geometrical curvature Ω_{de} takes the place of Ω_Λ. For the sake of completeness, we include $\Omega_k = 0$ in the equation, in order to express the perceived flatness of space. In the same way as in ΛCDM, $\Omega_{k,0} = 0$ describes the *flatness of space*, based on novel arguments, though, as it appears to us in our local reference frame as comoving FLRW observers.

In order to proceed with our approach, in an inflationary big bang cosmology, we allow for the following simplification. We analyze the evolution of cosmological models by the time inflation has ended and we call the expansion rate at the end of inflation "primordial expansion rate" (in analogy to the primordial power spectrum in structure formation). Detailed information of the exact evolution of H prior to this point is not required.

We recognize from Eq. (19)

$$\Omega_{\text{de},0} = 1 - \Omega_{\text{phys},0}, \tag{20}$$

where $\Omega_{\text{phys},0}$ denotes the sum total of the density parameters ($\Omega_{\text{CDM},0}$, $\Omega_{b,0}$, $\Omega_{r,0}$) of all physical contributions to the energy

budget of the universe (CDM, baryons, radiation; without consideration of the operationally defined contributions, $\Omega_{k,0}$ and $\Omega_{de,0}$, to the energy momentum tensor $T_{\mu\nu}$).

We rewrite the Friedmann equation (5), by multiplying Eq. (5) by $a^2(t)$ and divide it by 2, and where we use the total amount of energy $(4\pi/3)\rho_{phys}a^3$ in the sphere of radius (scale factor) a, in units of the critical density (see Eq. (20)), instead of the respective energy density ρ_{phys}, which yields

$$\frac{1}{2}\dot{a}^2(t) - \frac{G\Omega_{phys}}{a} = \kappa, \tag{21}$$

with the constant κ.

We use the EoS parameter of ρ_{de} to parameterize the dynamics of the expansion, determined by the curvature index in the FLRW metric, as a function of the sum total of the energy densities of the cosmic components in the Universe Ω_{phys}, which retains the customary ΛCDM formalism, while we are only left to adapt the computation of w_{de}.

So, we use now Eq. (21) to determine w_{de} as follows. Since κ is a constant, the evolution of the first term is determined by the evolution of the second term, given by

$$\frac{d}{da}\left(\frac{G\Omega_{phys}}{a}\right) \propto -\frac{\Omega_{phys}}{a^2}. \tag{22}$$

which is, unsurprisingly, equivalent to Eq. (14c). (In what follows, we do not need detailed prefactors.) We use relation (22) in Eq. (13) which yields

$$\rho_{de} \propto a^{-2\Omega_{phys,0}}, \tag{23}$$

and equate the exponents in (23) and $\rho_k \propto a^{-3(1+w)}$ [see Eq. (13)], rearranged to express w_{de} it reads as

$$w_{de} = \frac{2}{3}\Omega_{phys,0} - 1, \tag{24}$$

where w_{de} is constant.

The significant property of (24) is the fact that, in general, it does not yield the EoS of a cosmological constant. Only for an empty universe, we do *exactly* get $w_{de} = -1$. In fact, this is in nice accordance with the original *empty* de Sitter universe solution (de Sitter (1917)) and the expectations from a kinematically determined universe: If the universe is empty, there is no global curvature of space, and hence no deceleration, such that $H = const$, resulting in an exponential growth of the scale factor.

As soon as we have cosmic components, $\Omega_{phys,0} > 0$, the EoS parameter in (24) fulfills $w_{de} > -1$. If we choose the same matter content as the ΛCDM concordance model, i.e., using $\Omega_{phys,0} \simeq \Omega_{m,0} \simeq 0.3$, Eq. (24) yields $w_{de} \simeq -0.8$, thus there is a weak deceleration, compared to a model with $w_\Lambda = -1$. Still, the two EoS parameters are close numerically and in terms of their phenomenological impact onto the expansion history (see Section 6).

On the other hand, if we assume a universe at critical density, that is $\Omega_{phys,0} = 1$, yields $w_{de} = -1/3$, which is the EoS parameter of the spatial curvature used in the FLRW formalism, and which is restricted to the fine-tuned case of a universe at critical density. This is exactly what we expect.

To retain ΛCDM's formalism and Eq. (13), we make a distinction of cases. We apply the constant value of $w_{de} = -1/3$ to

flat and closed geometries, as is also the case in ΛCDM (with $w_k = -1/3$). For open geometries, we apply Eq. (24). In summary, we have

$$w_{de,early} = -\frac{1}{3} - \Theta(\Omega_{de,0})\frac{2}{3}\Omega_{de,0} \tag{25a}$$

$$\Omega_{de,0} = 1 - \Omega_{phys,0} \tag{25b}$$

where in Eq. (25a) Θ is the Heaviside function. The EoS parameter $w_{de,early}$ is a function of $\Omega_{de,0}$ [see Eq. (25b)], and therefore a *constant* for a given total of energy densities. We use the additional subscript "early" to express that this is the initial value for the EoS parameter in the early Universe. In Sec. 5, we will show that in the regime of nonlinear structure formation, the EoS will morph from a constant value to a time-dependent (or scale-factor-dependent) function. The Heaviside function separates the two regimes of super- and subcritical model universes. The first term corresponds to deceleration due to the critical density. The factor after the Heaviside function applies to subcritical universes only, where $w_{de,early}$ falls below $-1/3$, that is a decreasing EoS parameter implies less deceleration, as it should. In addition, we retain $\Omega_k = 0$ to express the perceived flatness of space, in our local inertial system (as comoving FLRW observers), just the same way as in ΛCDM. This is essential to linear perturbation theory applied in ΛCDM, when, for example, calculating the CMB temperature spectrum, as the notion "curvature" herein refers to spatial curvature in the Einstein equations (see e.g., Ma & Bertschinger (1995); Weinberg (2008); Coles & Lucchin (2002); Mukhanov (2005); Dodelson (2003); Peebles (1993)), and not to the geometry of the FLRW metric. A description of how the spatial curvature affects the CMB temperature spectrum can be found in many textbooks covering structure formation, see the aforementioned references. But there is a degeneracy for the impact of spatial curvature on the CMB spectrum with the cosmological constant Λ or dark energy, respectively; see for example, Hu & Dodelson (2002). We will get back to this point in Sec. 7.

Finally, the Friedmann equation reads

$$H^2(t) = \frac{8\pi G}{3c^2}\left[\rho_r(t) + \rho_b(t) + \rho_{CDM}(t) + \rho_{de}(t)\right] \tag{26a}$$

$$\rho_{de}(a) = \Omega_{de,0}\rho_{crit,0}\, a^{-3(1+w_{de,early})}, \tag{26b}$$

where Eq. (26b) now describes the evolution of ρ_{de} as a function of scale factor a for a constant $w_{de,early}$, given by Eqs. (25). The present-day critical density $\rho_{crit,0}$ is defined in (9).

Figure 1 finally displays the evolution of the scale factors of model universes with various matter densities, color-coded by density parameter Ω_m, whose value refers to the present, within our ΛCDM extension, from reddish for universes with closed geometry; the yellow one has exactly the critical density, that is the EdS universe, which separates the supercritical from the subcritical universes, which go from light green to deep blue for the empty universe. The curves between the yellow and the dark blue curve depict the evolution of subcritical models with matter densities between the EdS model with critical density (solid yellow curve), and the empty model (solid dark blue curve). We can see that the cosmological models transition uniformly between these two limiting model cases, corresponding to decreasing mass density, and "approaching" the exponential curve of the empty model, exactly as expected for kinematically determined universes in GR. In fact, a universe filled with a cosmological
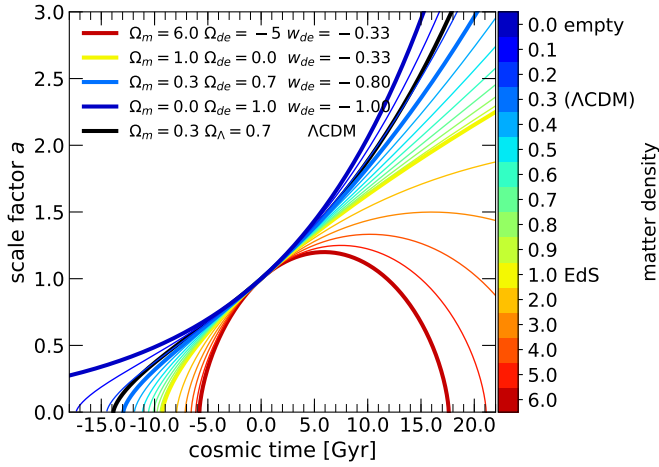
Fig. 1. Expansion histories of model universes within the ΛCDM extension. The color-coded curves display the expansion history of individual model universes applying Eq. (26), for models with supercritical density (dark red), to the EdS model (yellow), to the empty de Sitter universe (dark blue). The black curve indicates the expansion history of the original ΛCDM model with $\Omega_m = 0.3$, $\Omega_\Lambda = 0.7$, assuming a cosmological constant, i.e. $w_\Lambda = -1$. Comparing ΛCDM to the model shown for the same matter density and $\Omega_{de} = 0.7$ (thick light-blue curve), we see a great similarity. This model displays the same characteristic s-shape, indicating the transition from decelerated to accelerated expansion, because of $w_{de} = -0.8$ being "close" to a cosmological constant, given the relatively low energy density observed in the Universe.

constant to critical density displays the same evolution as the expectations for an empty universe, in the former by pressure balancing gravity[11], in the latter by vanishing gravity in an empty universe.

The black solid curve indicates the evolution of the ΛCDM model with $\Omega_m = 0.3$ and the cosmological constant $\Omega_\Lambda = 0.7$. Comparing it to the solution obtained by our ΛCDM extension with $\Omega_{de} = 0.7$ and $w_{de} = -0.8$ for a model universe with identical amount of matter $\Omega_m = 0.3$ (thick solid blue line), we recognize the similarity between both models. Both display the typical s-shape in the evolution of the scale factor, indicating the transition from decelerated to accelerated expansion, known from ΛCDM. There is a difference in the age between the two world models, however. We discuss this finding and other features, along with the results of exact calculations in Sec. 6. Moreover, the evolution of supercritical model universes with matter densities above the critical density match the expectation, as well. They display no deviations from conventional computations, with respect to the evolution of their scale factors.

This approach shows a significant difference to the cosmological constant Λ, that is considered a physical content of the Universe. But unlike the cosmological constant Λ, ρ_{de} now *does not* contribute to the energy budget of the Universe, instead it refers to a kinematic effect, described by an effective DE component emerging from the geometry of the FLRW metric. As such it is considered an operational contribution to the energy momentum tensor [Eq. (8)] and is not regarded as a physical contribution to the Universe. Just in the same way as ρ_k in ΛCDM, obviously. Though it seems to be only a minor modification, it is a signif-

---

[11]This scenario also applies to the inflationary phase of the Universe, when $p \approx -\rho$ of the inflaton field dominated the Universe, resulting in an exponential growth of the scale factor.

icant difference to the ΛCDM model, as the Universe, in this approach, is considered an open universe with subcritical energy density, as the sum total of the energy densities of the physical contributions (radiation and matter) to the energy budget of the universe is below critical density. Finally, $\Omega_{k,0} = 0$ refers to the perceived flatness of space in the local inertial system of the comoving FLRW observer, in contrast to ΛCDM, where it is interpreted as the global flatness of space.

5. The Expansion History in the Nonlinear Regime

In Sec. 4, we presented an extension to ΛCDM, which abandons the cosmological constant Λ in favor of an approach that describes the DE phenomenology as a kinematic effect, induced by the primeval expansion rate H_{ini} post big bang in relation to the initial density, in order to extend the ΛCDM model beyond the fine-tuned case of a Universe at critical density.

In ΛCDM, the nonlinear stage of structure formation is assumed to have no impact on the evolution of the background universe. In this section, we reassess the possibility of such an impact. More precisely, we investigate the impact of the formation of the cosmic web, in particular of its voids, onto the expansion history. We can show that there is an impact which is minor, but significant enough to explain the Hubble tension problem, on which we elaborate in detail below.

In order to motivate our approach, we reconsider first the ideas around the issue of a backreaction from structure formation, particularly in the late stages of the evolution of the cosmic web, since by then voids dominate the volume of the Universe.

5.1. The evolution of the voids

The pioneering work of Icke (1984) showed that voids evolve into spherical shape and become distributed homogeneously during the formation of the cosmic web. The following works by Icke & van de Weygaert (1987), van de Weygaert & Icke (1989) and van de Weygaert (1994) presented analytical descriptions of the evolution of the cosmic web, based on the Voronoi tessellation (Voronoi (1908), see also Okabe et al. (2000)). Icke & van de Weygaert (1991) confirmed the correctness of this approach by comparing it to observations. Analytical approximations are presented in Icke (2001), which describe the evolution of the individual components of the cosmic web as Voronoi features, which we display here

$$m_v = e^{-3\theta} \tag{27a}$$

$$m_w = 3e^{-2\theta}\left(1 - e^{-\theta}\right) \tag{27b}$$

$$m_f = 3e^{-\theta}\left(1 - e^{-\theta}\right)^2 \tag{27c}$$

$$m_n = \left(1 - e^{-\theta}\right)^3, \tag{27d}$$

where θ is a measure of time, with $\theta \propto t^{2/3}$ in an EdS universe. The quantities m_x denote the mass fractions of the individual components of the cosmic web: (a) m_v for the voids, (b) m_w for the walls, (c) m_f for the filaments and (d) m_n for the nodes.

As voids became a subject of interest, Colberg et al. (2005) and Shandarin et al. (2006) derived density profiles, shapes and sizes from cosmological simulations. Ricciardelli et al. (2013) showed that voids display a universal density profile. Cautun

et al. (2014) derived the evolution history of the individual components of the cosmic web from the Millennium simulation of Springel et al. (2005).

5.2. The backreaction problem

The expansion history of the Universe in the ΛCDM model is determined by the solution of the Friedmann equations, applying the average energy density of the background universe. This is a valid approach, as long as the distribution of the energy densities can be considered homogeneous and isotropic, that is in the early Universe. However, the cosmological principle is not valid anymore in the late Universe on spatial scales of the order of approximately Gpc and below. Thus, averaging the density of the Universe and solving the Friedmann equations by neglecting this nonlinear structure formation seems to be problematic. This is known in cosmology as the *averaging problem*. The theoretical background of this problem arises from the nonlinearity of the Einstein equations

$$E_{\mu\nu} = \frac{8\pi G}{c^4} \, T_{\mu\nu}, \tag{28}$$

first pointed out by Ellis (1983). Averaging the metric in an inhomogeneous environment first, before solving the Einstein equations, will lead to an additional correction term $C_{\mu\nu}$ in the averaged Einstein equations:

$$\langle E_{\mu\nu} \rangle = \frac{8\pi G}{c^4} \, \langle T_{\mu\nu} \rangle + C_{\mu\nu}. \tag{29}$$

The questions to be addressed are the following: (a) can this term reach relevant orders of magnitude to influence the expansion history of the Universe? (b) does perturbation theory eventually break down?

In ΛCDM it is assumed that the correction term $C_{\mu\nu}$ is negligible. On the other hand, if this term would be found to impact the expansion history, it would be seen as a *backreaction process*, caused by inhomogeneities onto the background universe.

The questions (a) and (b) have been explored in the literature, providing basically the following answers: in case the size of perturbations is much less than the (time-dependent) Hubble sphere, the correction term does not have substantial impact on the expansion history and can be neglected. This means it cannot explain the phenomenology of the accelerated expansion, see e.g. Kolb et al. (2005), Notari (2006), Li & Schwarz (2007), Räsänen (2006a), Buchert (2000, 2001), Kwan et al. (2009), Paranjape (2009).

Paranjape (2009) explored the averaging problem and its importance in cosmology in a mathematically rigorous way. They constructed a toy universe based on the Lemaître-Tolman-Bondi (LTB) metric (Lemaître (1933); Lemaître & MacCallum (1997); Tolman (1934); Bondi (1947)). The key property of this metric is that it allows radial inhomogeneities, while preserving isotropy. Their model was centered at an over-dense spherical region – a model for a formed dark matter halo –, surrounded by an underdense shell. The remaining part of the universe was regarded homogeneous out to the Hubble sphere. They found that the value of the correction term $C_{\mu\nu}$ induced by the inhomogeneity is too small, in order to have an impact onto the expansion history, justifying the assumptions of ΛCDM. However, while the toy model analyzed in Paranjape (2009) perfectly fits to the regime of halo formation and virialization, it does not apply to the late

stages of cosmic web formation, once voids dominate the volume of the Universe.

Buchert (2011) also investigated the averaging problem, based on the LTB metric, and finds that the global backreaction in a flat LTB model vanishes in a spherical domain. This result is compatible with the interpretation of the Universe to appear homogeneous, if we chose a large enough spatial scale, i.e. $\gtrsim$ 100 Mpc at the present (Hogg et al. (2005); Scrimgeour et al. (2012)), justifying the assumptions in ΛCDM. Moreover, Buchert & Ehlers (1997) have shown that in 3D-torus architecture global backreaction vanishes, as well, meaning that in cosmological simulations with periodic boundary conditions backreactions cannot appear.

5.3. The backreaction from voids

Although backreaction from the averaging problem has been shown to vanish in LTB models, Buchert et al. (2015) demonstrated that there is no proof that backreaction by inhomogeneities is negliglible, in general, in cosmology. Furthermore, it has been pointed out e.g. by Amendola & Tsujikawa (2010); Kolb et al. (2005) that the result of the averaging problem is very sensitive to the way the average is performed.

In this paper, we reconsider the averaging problem as applied to the late stages, when voids dominate the volume of the Universe. More precisely, we distinguish the impact of density vs volume. In the late stages of nonlinear structure formation, the Universe is dominated in volume by a homogeneous distribution of spherical voids of very low density, embedded in a highly over-dense region, which occupies only a minor fraction of the volume of the Universe. This picture is compatible with the general-relativistic "separate universe conjecture" (Weinberg (2008)), which states that a spherically symmetric region in a homogeneous and isotropic universe behaves like a mini universe. There are three approaches, which each can support the conjecture that voids as the dominating volume fraction of the Universe influence the expansion history: a) a phenomenological approach; b) a backreaction process; c) results of simulations; supported by d) results from observations, as discussed next.

a) phenomenological approach

Following the separate universe conjecture, every void can be considered a mini universe, having its own expansion rate. Moreover, we do not consider the evolution of a single void, but in a holistic view, we consider the entire Hubble sphere.

The expansion rate of the Universe decreases with time, due to the action of gravity. This deceleration is determined by the gravitational forces F_G between any two points (p_1, p_2) in the homogeneous universe. Following Birkhoff's theorem (Birkhoff & Langer (1923); Jebsen (1921, 2005); Maciel et al. (2018)), gravitational forces in a homogeneous sphere are proportional to the distance r between any point p from the center p_c: $F_G \propto r(p, p_c)$. Considering points p_x at the edge of a over-dense region surrounding a very under-dense void, yields the usual Newtonian law of gravity $F_G \propto 1/r^2(p_x, p_c)$. This can be applied to the scenario, where voids are embedded in an over-dense environment, showing that deceleration in the voids is less pronounced than in the surrounding cosmic web. Alternatively, this can also be seen by the Birkhoff's theorem for the spherical low-density voids, yielding a lower gravitational force within the voids compared to their higher-density homogeneous environment. This means that voids are experiencing an accelerated expansion, compared

to their higher-density homogeneous environment. As long as voids do not dominate the volume of the Universe, this expansion can be compensated by the "congestion" of the over-dense walls and filaments. As soon as voids begin to dominate the volume of the Universe, this compensation fails. Voids dominate the volume of the Universe and therefore the expansion of the Universe, as it is directly connected to the volume of the voids.

b) backreaction process

The solutions to the averaging problem which we present in Sec. 5.2 consider the size of inhomogeneities clearly smaller than the Hubble radius. Therefore, it is always possible to find a minimum spatial scale, above which the Universe can be considered homogeneous, yielding no impact on the expansion history.

However, as studies have shown, in case perturbations are of the size of the Hubble radius or even larger ("superhorizon modes"), the correction term can grow to significant values, and therefore may impact the expansion history of the Universe, which appears as a classical (zero-momentum) background (see e.g. Carloni et al. (2008), Martineau & Brandenberger (2005), Barausse et al. (2005), Kolb et al. (2005), Parry (2006), Kumar & Flanagan (2008), Hirata & Seljak (2005), Flanagan (2005), Räsänen (2006b), Geshnizjani et al. (2005)). This topic is subject to controversial discussions, and it has been even questioned if such huge perturbations exist at all (see e.g. Carloni et al. (2008), Stoeger et al. (2007), Wetterich (2003), Calzetta et al. (2001), Siegel & Fry (2005), Gasperini et al. (2009), Gruzinov et al. (2006), Notari (2006), Van Acoleyen (2008)).

Yet, relativistic perturbation theory does predict superhorizon perturbations, and as the Hubble sphere grows over time, more and more such perturbations enter that sphere (perturbations leave the sphere, once the scale factor grows exponentially and $H = const$). Either way, it appears that these superhorizon perturbations are far too subdominant to source a backreaction process onto the background evolution, in order to explain the phenomenology of the accelerated expansion.

In our model, we take into account the evolutionary stage of the cosmic web, once voids dominate the volume of the Universe, that is low-density spherically symmetric voids are embedded in a highly over-dense homogeneous background. Furthermore, we consider the impact of the entire cosmic web on the backreaction process, meaning we consider the entire Hubble sphere. Therefore, we can regard the entirety of all voids as *one* huge extreme low-density region – appearing as a classical (zero-momentum) background, see for example, Barausse et al. (2005), Kolb et al. (2005)).

c) backreaction via spatial averaging

Let us add another aspect of the backreaction. In Buchert et al. (2015) it was shown that, in general, there is no proof that inhomogeneities are negligible in background cosmology. Nevertheless, the success of the ΛCDM model suggests that any impact of inhomogeneities on the expansion rate should be weak. However, in Wiltshire (2007, 2011) it was shown that particularly in the late stages of the evolution of the cosmic web, averaging and coarse-graining is a problematic procedure.

Rácz et al. (2017) performed a cosmological N-body simulation, integrating the Newtonian equations, as is customary in cosmological simulations (e.g., Springel et al. (2005)), with a changing general-relativistic metric, which is calculated from spatially averaged quantities. The result indicated that for a typical spatial scale of the averaging procedure, an impact onto the expansion history with deviations from the results based on the FLRW metric is possible.

Before we close this section, we reiterate that all studies indicate that the backreaction onto the background evolution, including the backreaction from voids, cannot "explain away" the phenomenology of accelerated expansion. However, by including the minor backreaction of voids that we find, we can possibly resolve the Hubble tension problem, as shown below.

d) results from observations

As discussed in a later section, recent work by e.g., Dainotti et al. (2022b, 2021, 2022a); Bargiacchi et al. (2023b,a); Ó Colgáin et al. (2021) and Krishnan et al. (2021), indicate that the evolution of the expansion rate H at low redshift is in conflict with the assumption of a cosmological constant. These results may indicate that the origin of the Hubble tension is likely to be in cosmology and not in local measurement issues, where a dynamical DE component, our proposed model, or a backreaction from the late stages of structure formation might each a priori constitute a solution.

5.4. Including Backreaction into the ΛCDM Extension

There is a straightforward approach to incorporate the backreaction from the cosmic web and its voids into the ΛCDM extension, and at the same time to quantify the corresponding impact onto the expansion history, as follows. We apply the hydrodynamical and geometrical models from Icke (1984), Icke & van de Weygaert (1987) and Icke (2001) for the formation of the cosmic web and extract the relevant quantities from the analysis by Cautun et al. (2014) of the Millennium simulation. The advantage of this procedure is the fact that the large-scale structure of the Universe in our model is informed by cosmological ΛCDM simulations, which are in good agreement with observations, that is with large galaxy surveys on scales of the cosmic web.

In the ΛCDM extension, which we presented in Sec. 4, the cosmological constant Λ is replaced by an "operational dark energy", where the associated EoS is given in Eqs. (25). As previously mentioned, the expansion of the voids is directly connected to the expansion of the Universe by their dominance in volume and their low density. Therefore, it is straightforward to express the impact from voids onto the expansion history through the EoS of ρ_{de}. As a result, the initially constant EoS parameter $w_{de,early}$ morphs into a time-dependent function. This makes sense, because voids become important only at the later stages of structure formation. To quantify this effect, we used the results derived by Cautun et al. (2014), who analyze the evolution of the cosmic web and who derive the evolution of the mass fractions and volume fractions for the individual components of the cosmic web (i.e., voids, filaments, walls, nodes), using the Millennium simulation by Springel et al. (2005). Cautun et al. (2014) find that voids dominate the volume of the Universe as of a redshift $z \sim 5$. The analytical model (27) from Icke (2001) shows that the matter fraction of the voids evolves linearly in redshift, to a good approximation, in the late stages of the evolution of the cosmic web. We applied both findings to our Eqs. (25), in order to derive the following linear approximation for the evolution of the EoS parameter of ρ_{de} as a function of the scale factor as follows. We use Eqs. (25) to obtain the $w_{de,early}$ (from parameters reported by the Planck-Collaboration (2020)) and $w_{de,0}$ (from the

results reported by Cautun et al. (2014)). In the linear evolution of redshift from $z = 5$ to $z = 0$, we use $z + 1 = 1/a$ to express w_{de} as a function of scale factor a, which yields

$$w_{de}(a) = \begin{cases} w_{de,early} & \text{when } a \le 1/6 \\ w_{de,early} + \left[\frac{(1/a-1)-5}{5}\right](w_{de,early} + 0.9) \\ & \text{when } a > 1/6. \end{cases} \quad (30)$$

Thus, the EoS parameter w_{de} becomes a function of cosmic time, or scale factor, respectively, as indicated in the formula, once the scale factor has reached the threshold determined by the aforementioned analysis. Using the density parameters of our model with $\Omega_{de,0} = 0.7$ and $\Omega_{m,0} = 0.3$, we get for the present-day EoS parameter $w_{de}(1) \sim -0.9$. Comparing this result with the constant EoS parameter $w_{de,early} = -0.8$ of Sec. 4, we see that the impact of voids leads to a more negative EoS parameter, with a value closer to that of a cosmological constant. In fact, this is an expected outcome, given the dynamics of voids.

In order to reflect the correct evolution of the background, we stress that the time-dependence of the EoS parameter requires a forward-in-time-integration of the energy conservation equation (11) to determine the evolution of the energy density ρ_{de}. Thus, Eqs. (13) and (26b), respectively, cannot be used naively. Regarding this important point, we refer the reader to Foidl & Rindler-Daller (2024), where we discuss in detail computational characteristics for cosmological models with a dynamical dark energy component and the implications of a decreasing vs increasing EoS parameter.

We mentioned already that the impact of voids makes the EoS parameter w_{de} more negative, than without this impact. In fact, as the density within voids decreases while their volume increases, $w_{de}(a)$ will converge asymptotically to the EoS parameter $w_{de} = -1$ of a cosmological constant.

6. Results for the wCDM Extension to ΛCDM

In order to calculate accurately the background evolution of our ΛCDM extension, and to compare it carefully with the concordance ΛCDM model and with observations, we use the open-source cosmological Boltzmann code CLASS [12], which is designed, not only to provide a user-friendly way to perform cosmological computations, but also to provide a flexible coding environment for implementing customized cosmological models. The modular concept makes it possible to enhance the code, without the risk of compromising existing functionality. The underlying concepts, including an overview of coding conventions, can be found in Lesgourgues (2011). This version uses the Planck 2018 cosmological parameters from Planck-Collaboration (2020), as the default parameter set. Additionally, the configuration provides different sets of precision configuration files, to reflect varying requirements on precision, which may be needed in the results or available computation time. The precision configuration with the highest accuracy is proofed to be in conformance with the Planck results within a level of 0.01%.

We use the fiducial parameters of the ΛCDM model from Planck-Collaboration (2020), shown in Table 1, in our calculations. We properly implemented the equations of our ΛCDM

---

[12] The code CLASS is publicly available at https://lesgourg.github.io/class_public/class.html

extension (25), (26) and (30) into the background module of CLASS, as well as into the perturbation module, because we also calculated and compared the CMB temperature spectra between our ΛCDM extension and concordance ΛCDM, as presented in the course of the next section.

Table 1. Cosmological parameters used in the computations

| Parameter	Value	Comment
H_0	67.556	
T_{CMB} [K]	2.7255	
N_{ur}	3.046	
$\Omega_{\gamma,0}$	5.41867×10^{-5}	derived from T_{CMB}
$\Omega_{\nu,0}$	3.74847×10^{-5}	derived from N_{ur}
$\Omega_{b,0}$	0.0482754	
$\Omega_{CDM,0}$	0.263771	
$\Omega_{de,0}, \Omega_{\Lambda,0}$	0.687762	wCDM, ΛCDM
$\Omega_{k,0}$	0	
τ_{reio}	0.0925	
A_s	2.3×10^{-9}	
n_s	0.9619	adiabatic ICs

In order to compare the results of our ΛCDM extension to the concordance ΛCDM model, two CLASS simulations were run. The first run was performed using the unmodified version of CLASS. The second run used our amended version of CLASS with parameters according to Table 1. In what follows, we designate the cosmological constant by Λ, as customary. The effect of DE in the ΛCDM extension, we denote by ρ_{de}, w_{de} and Ω_{de}, respectively, for habit's sake; see Sec. 4. ΛCDM refers to the concordance model, whereas the ΛCDM extension is denoted as "wCDM". This notion is often associated with the specific CPL parametrization (1), whereas we use it to refer to our own parametrization in (30).

6.1. Evolution of densities and equation of state

Figure 2 displays the evolution of the energy densities ρ_i vs scale factor a, as well as vs proper time, in both models. The top panel displays the evolution of the densities in the ΛCDM model, corresponding to the individual components of the Universe, as indicated in the legend. The slopes of the individual curves are as expected from Eqs. (14). The red solid line depicts Λ, showing a constant evolution as expected for the cosmological constant. The bottom panel displays the evolution of the energy densities in the wCDM model. In this model, the early slope of the red curve for ρ_{de} corresponds to the EoS parameter $w_{de,early} \simeq -0.8$, determined by (25) and (30). The vertical lines in blue bracket the epoch of big bang nucleosynthesis, between neutron-proton freeze-out at $a_{n/p} \sim 1.3 \times 10^{-10}$ and nuclei production at $a_{nuc} \sim 3.3 \times 10^{-9}$, while the vertical lines in red (at larger scale factor) indicate the time of matter-radiation equality $a_{eq} \sim 10^{-4}$, followed by recombination $a_{rec} \sim 10^{-3}$ (the detailed numbers for the latter depend somewhat more upon the cosmological model). The effect of the backreaction from voids in the late stages of the evolution is so small that it cannot be recognized in the log-log plot. The evolution of the matter and radiation components indicates no significant differences between the two models, as expected.

However, the ages of the models differ, as can be seen from the value of the proper time at the very present. The ΛCDM model has an age of 13.8 Gyr, whereas the age of the wCDM model
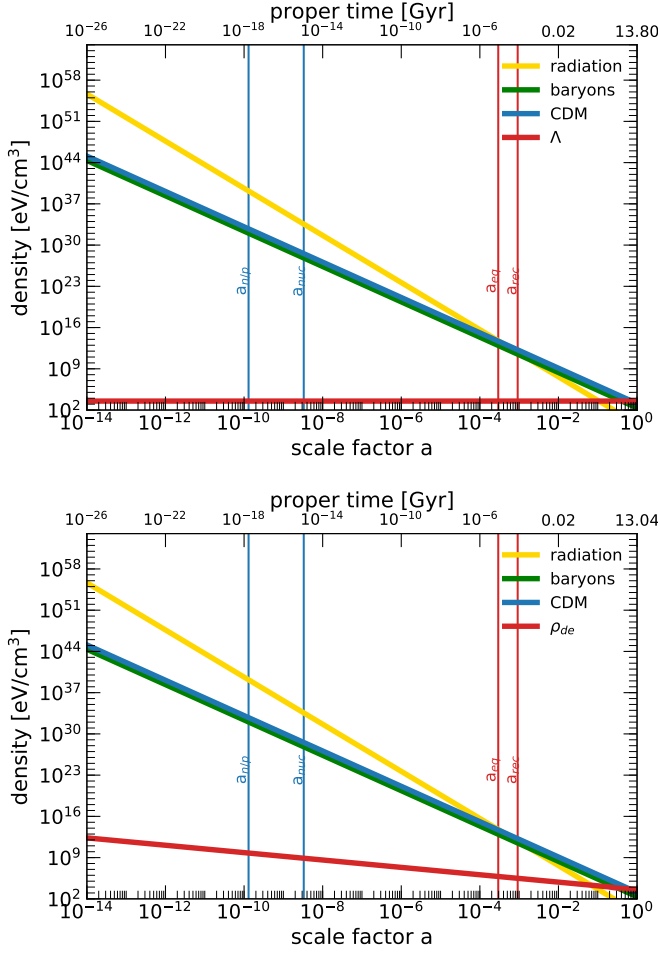
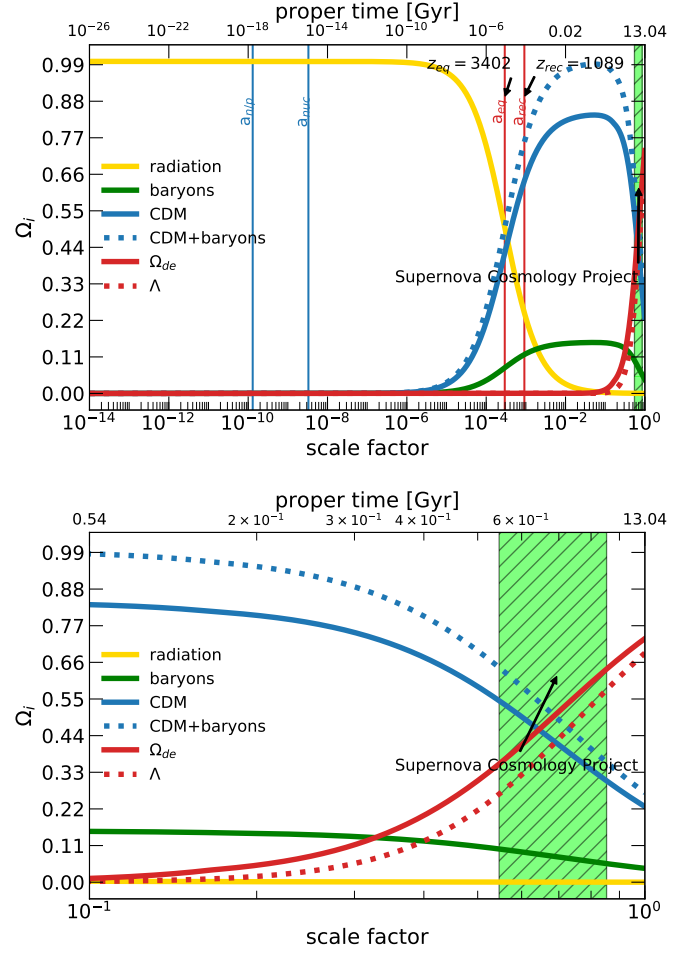**Fig. 2. Evolution of energy densities in ΛCDM (top panel) and wCDM (bottom panel) as a function of scale factor and proper time, respectively.** The top panel displays the evolution of the individual contributions to the energy density of the ΛCDM model according to (14). The red solid line indicates the evolution of the cosmological constant Λ. The bottom panel displays the evolution of the individual contributions to the energy densities of the wCDM model. The radiation and matter components show no differences, compared to ΛCDM. However, the red solid line for ρ_{de} is not a constant, but has a slope, corresponding to $w_{de,early} \sim -0.8$, according to (25). Note that the late impact of voids onto $w_{de,early}$ is not recognizable in the log-log plot. The vertical lines in blue bracket the epoch of big bang nucleosynthesis, between neutron-proton freeze-out at $a_{n/p} \sim 1.3 \cdot 10^{-10}$ and nuclei production $a_{nuc} \sim 3.3 \cdot 10^{-9}$, while the vertical lines in red (at larger scale factor) indicate the time of matter-radiation equality a_{eq}, followed by recombination a_{rec} (see also Fig. 3).

Fig. 3. Evolution of density parameters in ΛCDM and wCDM. The top panel displays the evolution of the density parameters in the wCDM model vs scale factor and proper time, respectively. It includes also Ω_Λ of the ΛCDM model (red dotted curve) in order to compare it to Ω_{de} (red solid curve) of the wCDM model. Vertical lines are the same as in Fig. 2. The bottom panel displays the same quantities but shows a zoom-in to highlight the range of scale factors from $a = 0.1$ to 1. We see that Ω_{de} of wCDM gets dominant earlier than Ω_Λ of ΛCDM, but that toward $a = 1$ the two curves come closer again. As an illustration, the green-hatched vertical band indicates the range of scale factors of the sample of galaxies used by the Supernova Cosmology Project (Perlmutter et al. (1999)). More explanations can be found in the main text.

is 13.04 Gyr. In Sec. 6.3, where we discuss the Hubble tension problem, we will present arguments to show that the lower age of the wCDM universe is no obstacle for the model.

Figure 3 displays the evolution of the density parameters Ω_i (as indicated in the legends) vs scale factor a and proper time, respectively, for both models. The panels display both Ω_{de} of wCDM (red solid curve) and Ω_Λ of ΛCDM (red dotted curve). We can see that Ω_{de} of wCDM gets to be the dominant contribution to the energy budget of the Universe at a smaller scale factor than Ω_Λ of ΛCDM. As an illustration, we include the green-hatched vertical band which indicates the range of redshifts (resp. scale factors) of the sample of galaxies used by the Supernova Cosmology Project (Perlmutter et al. (1999)). It was

one of the high-redshift SNe Ia surveys that discovered the accelerated expansion in the late 1990s. The bottom panel displays the same quantities but shows a zoom-in to highlight the range of scale factors from $a = 0.1$ to 1. While the advanced Ω_{de} gets dominant earlier than the cosmological constant Λ, the two curves come close again at larger a, due to the backreaction from voids which makes ρ_{de} converge to a cosmological constant.

In Figure 4 we show the evolution of the effective EoS parameter for ΛCDM and our wCDM model, respectively. The *effective* EoS parameter $w_{eff}(t) = p_{tot}(t)/\rho_{tot}(t)$ is determined by the time-dependent sum of pressures and densities of all cosmic components. (Generally, if one component dominates strongly over the others, w_{eff} is close to the EoS parameter of that component.) In the top panel with the scale factor on the lower x-axis, we recognize the early radiation-dominated phase, where $w_{eff} = 1/3$ to high accuracy. In terms of cosmic time on a linear

x-axis scale in the bottom panel, this phase is so short that it is seen as a vertical bar along the y-axis. Once matter strongly dominates in the Universe, shortly after a_{eq}, w_{eff} drops to zero. In the latest phase, when Λ begins to dominate the Universe in ΛCDM, the effective EoS parameter drops to its present-day value of $w_{eff} \sim -0.7$. On the other hand, in the wCDM model, the effective EoS parameter initially decreases more rapidly, compared to ΛCDM. Only by the time the backreaction from voids comes at play in wCDM, the evolution approaches the one of ΛCDM, around the present, which can be also seen in the bottom panel of the figure.

In that bottom panel, we also highlight the evolution of the effective EoS parameter w_{eff} in the far future for the two models. We can see that, as of a cosmic time of $t \sim 22$ Gyr, the w_{eff} in both models, ΛCDM and wCDM, will show no significant difference, and w_{eff} will be very close to -1 by the time of $t \sim 28$ Gyr for ΛCDM and $t \sim 31$ Gyr for wCDM. However, while the dominance of Λ as a cosmological constant is attributed to the former, it is the (relic) kinematic effect of the big bang via H_{ini} in relation to the initial density, respectively, that is responsible for the dominance of ρ_{de} in the latter model.
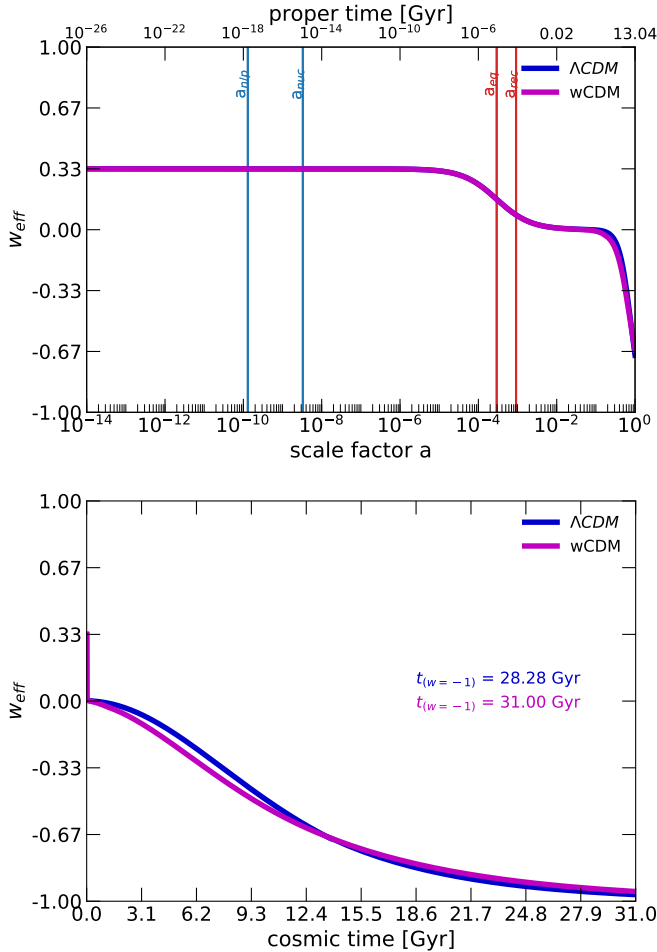
Fig. 4. Evolution of effective EoS parameter w_{eff} in extended and concordance ΛCDM. The top panel displays the evolution of w_{eff} in both models vs scale factor and proper time, respectively, with the same vertical lines as in Fig. 2. The bottom panel displays w_{eff} vs cosmic time in linear scale! The cosmic time when $w_{eff} \simeq -1$ is indicated in the plot; it amounts to $ct = 28.28$ Gyr for ΛCDM vs 31.0 Gyr for the ΛCDM extension, respectively.

6.2. Expansion history

Figure 5 shows the expansion history of ΛCDM and wCDM. The top panel displays the growth of the scale factor a with cos-
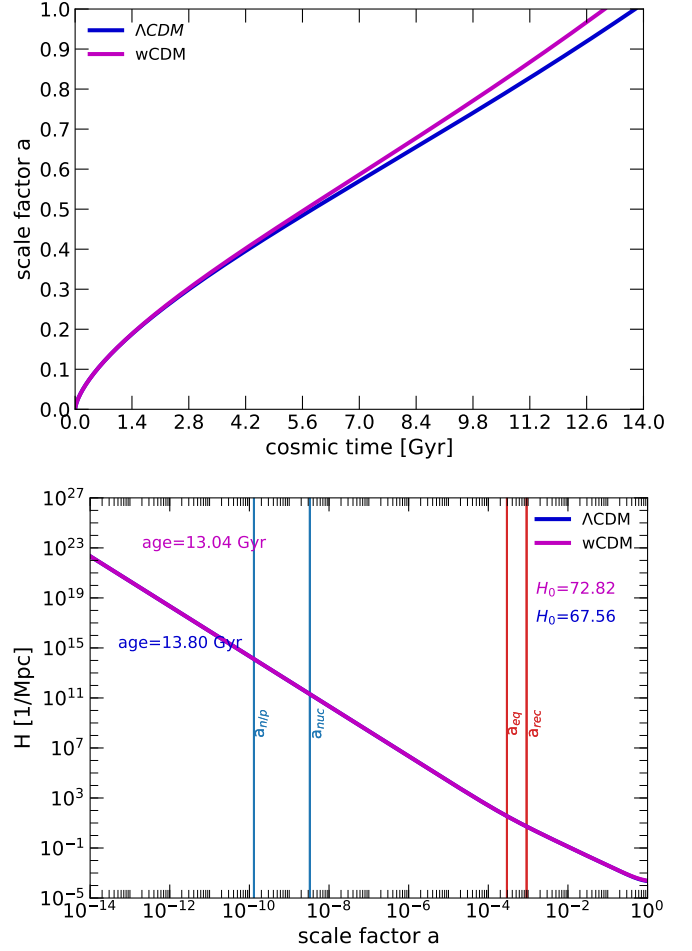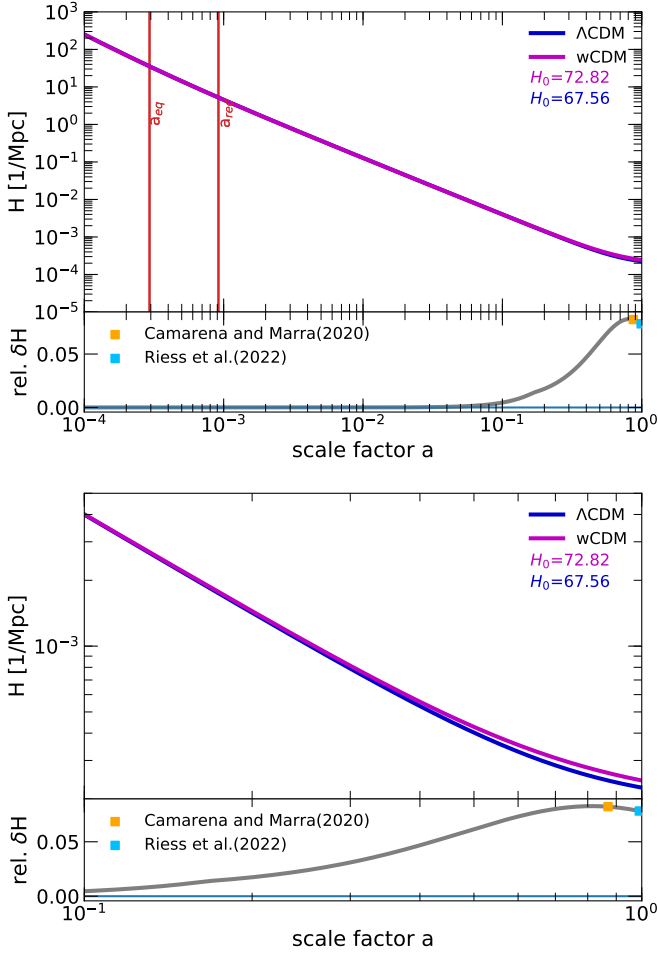

Fig. 5. Evolution of scale factor and Hubble parameter in ΛCDM and wCDM. The top panel shows the evolution of the scale factor vs cosmic time for ΛCDM (blue curve) and wCDM (magenta curve); note the linear scales in this plot. The wCDM model expands faster than the ΛCDM model, which can be better recognized in Fig. 6. The bottom panel shows the evolution of the expansion rate or Hubble parameter H (displayed in CLASS conventions in units of $1/$Mpc) vs scale factor for both models. Its present-day value H_0 differs: ΛCDM has $H_0 = 67.56$ km/s/Mpc, whereas wCDM has $H_0 = 72.82$ km/s/Mpc. Vertical lines in the bottom panel are the same as in Fig. 2.

mic time t in linear scale for both models. The bottom panel shows the evolution of the Hubble parameter (i.e., expansion rate) H vs scale factor a. In wCDM the scale factor grows faster than in ΛCDM. This results in a younger age of 13.04 Gyr for wCDM, compared to 13.80 Gyr for ΛCDM.

The present-day value of the expansion rate, the Hubble constant H_0, also differs between the two models: ΛCDM has a value of $H_0 = 67.56$ km/s/Mpc and wCDM has $H_0 = 72.82$ km/s/Mpc. Of course, the value for ΛCDM is informed by CMB measurements from Planck, and is part of the parameters provided by CLASS, see Table 1.

Now, in order to illustrate the late impact by voids onto the expansion history of wCDM, compared to ΛCDM, Figure 6 shows zoom-ins of the evolution of the expansion rate H for $a \geq 10^{-4}$

Fig. 6. Evolution of Hubble parameter vs scale factor The top panel shows the evolution of the expansion rate H vs scale factor for ΛCDM (blue curve) and the ΛCDM extension (magenta curve) and their relative deviation as the gray curve in the bottom of each panel. The panels just differ in the range of scale factors shown. In the bottom panel, it can be recognized that the ΛCDM extension expands faster than ΛCDM. The orange and the blue filled square indicate measurement values of H_0 by Camarena & Marra (2020) and Riess et al. (2022), respectively. The red vertical lines in the top panel are the same as in Fig. 2. In our wCDM model, the Hubble parameter H increases by ∼ 8 % by the present, compared to that of ΛCDM. As a result, the model provides an explanation for the Hubble tension problem and agrees with H_0-measurements at different redshifts.

(top panel) and $a \geq 10^{-1}$ (bottom panel). The vertical red lines indicate the scale factor at matter-radiation equality a_{eq} and at recombination a_{rec}, respectively. The gray solid curve at the bottom of each panel displays the relative deviation of H in wCDM from its value in ΛCDM. We can clearly see that at the time of recombination, when the CMB was emitted, there is no difference in H between the models. However, at the late stages of the evolution, once the impact of the formation of the cosmic web becomes relevant, the expansion rate in the wCDM model increases. At a scale factor of $a \sim 0.8$, the deviation reaches a maximum, but then decreases, yielding a value of $H_0 = 72.82$ km/s/Mpc. The bottom panel exemplifies this even more clearly. Again, this shift to a higher value of H_0 by ≈ 8% is due to the backreaction caused by voids. The origin of the rise of H_0 in our ΛCDM extension is the time-dependence (scale-factor dependence) of the EoS parameter $w_{de}(a)$. As mentioned earlier,

we cannot use the customary procedure applied in ΛCDM to determine the energy density ρ_{de} via (13), as the EoS parameter $w_{de}(a)$ is not a constant anymore. Hence, we have to perform a forward-in-time integration of ρ_{de} by integrating (11), to solve the Friedmann equation (8), which we discuss in detail in Foidl & Rindler-Daller (2024). The consequence of this integration is that, as $w_{de}(a)$ decreases with time, it leads to a rise in the value for H_0, and this value is higher compared to the parameterized Planck value given in Table 1. As a result, the ΛCDM extension can explain the Hubble tension problem, on which we elaborate below.

6.3. The Hubble Tension and σ_8-Tension

Our wCDM model of the previous section is phenomenologically similar to models of quintessence or "early dark energy" (EDE), which also propose solutions to the Hubble tension problem. A review on these models is given in Poulin et al. (2023). The Hubble tension problem refers to the reported discrepancy between the values[13] of H_0 derived from measurements of the CMB vs those derived from measurements in the "local" Universe, using standard candles such as SNe Ia or Cepheid variables. The measurements in the local Universe consistently reveal a higher value of H_0, than the measurements of the CMB. This problem is discussed for example in Di Valentino et al. (2021), where two measurement values in the local Universe are of particular interest to us for a comparison with our ΛCDM extension (see their Fig. 1 and the bottom parts of both panels of our Figure 6): Riess et al. (2022) with $H_0 = 73.04$ km/s/Mpc and Camarena & Marra (2020) with $H_0 = 75.4$ km/s/Mpc. The wCDM model with its value of $H_0 = 72.82$ km/s/Mpc agrees quite well with the value determined by Riess et al. (2022). The result of Camarena & Marra (2020) seems to be an outlier, as their H_0-value is even higher. The explanation for this can be found in the redshift range of the respective samples of galaxies for these two measurements. The redshifts of the sample used in Riess et al. (2022) lie between $z = 0.011$ and $z = 0.02$, whereas the sample in Camarena & Marra (2020) is in a range between $z = 0.023$ and $z = 0.15$. Yet, because wCDM exemplifies a higher value of H around that same epoch, it can also explain the results of Camarena & Marra (2020), whose measurement neatly lies on the maximum of the deviation of H in the wCDM model, compared to ΛCDM, see Figure 6. This result came quite as a surprise when we studied this comparison in detail.

Now one of the drawbacks of these attempts is that mitigating the Hubble tension problem increases the σ_8 tension (see e.g. Kamionkowski & Riess (2023)), which has emerged in recent years. This is a measure of the homogeneity of the Universe, where S_8 is defined as $\sigma_8 \sqrt{\Omega_m/0.3}$, with σ_8 being the standard deviation of the density fluctuation in a sphere of radius $8\,h^{-1}$ Mpc. A disagreement of more than 4σ has been found between the extrapolation of the CMB temperature fluctuations forward to the present day, and what is measured by multiple probes of the inhomogeneity in the nearby Universe: The value of S_8 derived from the CMB is higher than that observed in the local Universe. A mitigation of the Hubble tension (i.e., by increasing H_0) increases the σ_8 tension. In Rebouças et al. (2024), this was addressed by assuming a modification of EDE in the late universe, which provides a solution to both problems. However, the

---

[13]Strictly speaking, H_0 refers to H at $z = 0$, but since the community casually uses the notation H_0 also for any H at low $z \lesssim 1$, we stick to this convention.

modifications to EDE are purely empirically motivated, whereas our wCDM model is based upon a consistent set of physical processes involved in the evolution of the Universe.

In addition, we find that our $S_8 = 0.784$ almost exactly matches the value of the DES-Y3 measurements for which $S_8 = 0.782 \pm 0.019$, by assuming a constant neutrino mass $\sum M_\nu$. The final data release by the Planck mission in Tristram et al. (2024) also compares their result to this value. The result is in agreement with the findings by Rebouças et al. (2024), who found that a time-dependent $w(z)$ at late times, can resolve Hubble tension *and* σ_8-tension. Indeed, this is the case in our extension wCDM, because the evolution of $w(z)$ in our model is constant in the early Universe, but in the late stages, it becomes a time-dependent function.

Now, in order to investigate whether the lower age of the wCDM model constitutes a problem, we compare some age indicators from the literature, notably estimates for the ages of the oldest known stars in the Universe. Their ages are estimated basically via two different methods: the abundance of heavy elements, mainly those formed by the r-process in core collapse supernovae; the second way is the determination of the time of the main sequence turn-off of metal-poor stars in globular clusters. A short review of methods and observations is given in Weinberg (2008), with age estimates of the oldest stars between 11.5-14 Gyr, where the error bars are ~ 2 Gyr. The observations of metal-poor galaxies by Grebel (2012) and globular clusters in the local Universe by Grebel (2016) display consistent results, albeit with larger error bars of $2 - 4$ Gyr. A more recent observation, based on the age of the metal-poor globular cluster NGC 6397 using WFC3/IR photometry is given in Correnti et al. (2018), showing a similar age range with smaller error bars of 12.6 ± 0.7 Gyr. All these results are consistent with the age of our wCDM model.

For comparison's sake, we also computed the age of a ΛCDM universe using H_0 from Riess et al. (2022), while keeping the other parameters unchanged: the result is 12.50 Gyr. This age for ΛCDM would also be still on the save side with respect to the age estimates of the oldest known stars.

Cimatti & Moresco (2023) follow a different approach. They select the oldest objects from the literature and perform a statistical analysis within a ΛCDM cosmology, in order to determine the upper limit of H_0 compatible with the ages of the selected objects. They find $H_0 < 73.0 \pm 2.5$ km/s/Mpc with a probability of 93.2 %. So, the "Riess model" is just within these constraints. Since the expansion rate in wCDM increases only later in time, it is less affected by this upper limit.

Let us also comment on the early galaxies which have been found recently by the James Webb Space Telescope, see Curtis-Lake et al. (2023), Finkelstein et al. (2023) and Robertson et al. (2023). It has been estimated that these galaxies have formed only about 320 million years after the big bang. However, we stress that such estimates require the adoption of a specific cosmological model, in order to convert the measured redshifts into an age. Adopting a ΛCDM model with the H_0 determined by the Planck telescope, or the H_0 determined from the local Universe (e.g. by Riess et al. (2022)), will in each case shift the age of the galaxies accordingly, and the same is true if we adopt the wCDM

model, instead. In each case, there is no conflict between the age of these model universes and those early galaxies[14].

Recent studies by e.g., Dainotti et al. (2022b, 2021, 2022a); Bargiacchi et al. (2023b,a); Ó Colgáin et al. (2021) and Krishnan et al. (2021), indicate that the evolution of the expansion rate H at low redshift is in conflict with the assumption of a cosmological constant, and dynamical models of DE seem to be preferred. These results may indicate that the origin of the Hubble tension is likely to be in cosmology and not in local measurement issues (e.g. Krishnan et al. (2021)), as observations with increasing accuracy of H_0 in the local Universe seem to exacerbate the Hubble tension (e.g. Dainotti et al. (2023) and Khalife et al. (2024)). The evolution of the expansion rate, shown in Figure 6, displays a peak in the deviation to ΛCDM at $a \sim 0.8$. In fact, the position of this peak seems to be characteristic for individual DE candidates; see Foidl & Rindler-Daller (2024).

7. Results for the owCDM Extension to ΛCDM

In the course of this section, we fit the wCDM model to the ΛCDM CMB spectrum as well as to the value $H_0 = 73.04$ km/s/Mpc, derived by Riess et al. (2022), giving the owCDM model. In CLASS, we can readily incorporate the equations for wCDM, not only in the background module, but also in the perturbation module, in order to calculate perturbation spectra. Except for Ω_Λ, wCDM uses the same cosmological parameters as concordance ΛCDM (see Table 1). Also, it is based upon the standard CDM framework, concerning its matter content and the cosmic web (and void) structure. Therefore, we expect no big differences in the perturbation spectra between wCDM and concordance ΛCDM. In fact, the output by CLASS confirms this expectation, see Fig. 7, where we show the power spectrum of the CMB temperature anisotropies of the wCDM and the ΛCDM model.
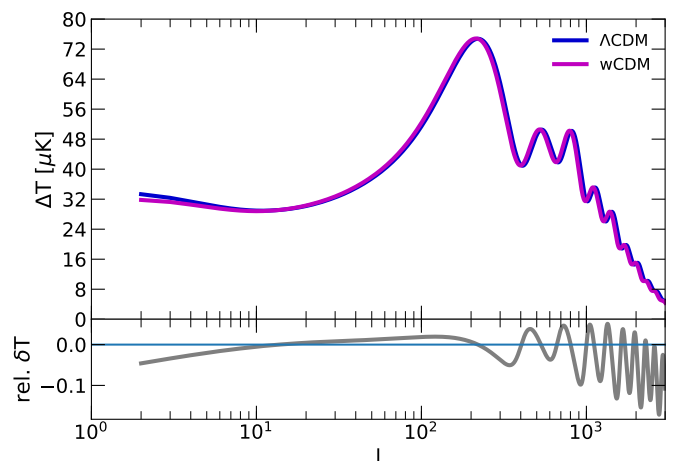
Fig. 7. The CMB temperature power spectrum in ΛCDM (blue) and in our wCDM model (magenta). The relative differences are shown at the bottom of the panel, and amount to ~ 15 %.

Although we see no significant differences in the structure of the peaks in the CMB temperature power spectrum, the deviations are at a ≲ 15% level. The structure of the peaks is almost
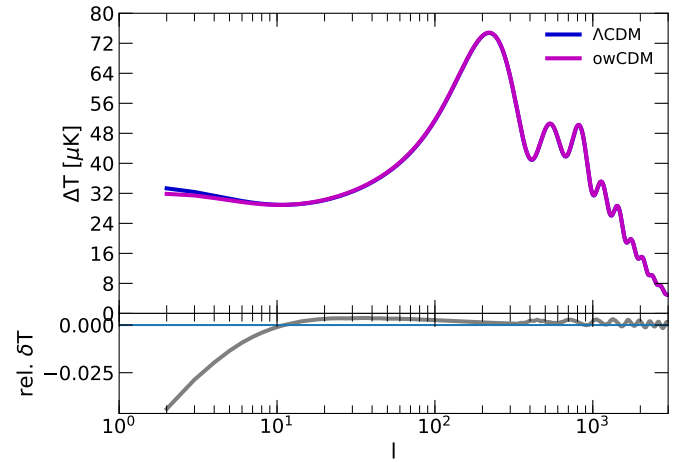
---

[14] Or, rephrased, all these cosmological models face a potential challenge in explaining the early formation of these galaxies.

identical, but the peaks are slightly shifted to the left, which can be explained as follows. The amplitudes of the peaks in the spectrum are determined by the density parameters $\Omega_{\gamma,0}$ for radiation, and $\Omega_{b,0}$ and $\Omega_{CDM,0}$ for the matter components. The relative height of the peaks is determined by the ratio of $\Omega_{b,0}$ and $\Omega_{CDM,0}$. Hence, it is obvious that the structure of the peaks is in agreement with ΛCDM, as we used the concordance values for these density parameters. However, the parameterization of DE impacts the expansion rate, as exemplified in Sec. 6.2. Since there is no interaction between DE and the other cosmic components, the replacement of DE for Λ does not impact the structure of the peaks. Keeping in mind that the multipole moments, shown on the x-axis, are in Fourier space, however, explains the shift of the spectrum to the left-hand side. More precisely, it is not a shift, but rather a stretching (compressing) of the spectrum from the right-hand side to the left-hand side, with increasing (decreasing) expansion rate. Thus, the slightly higher value of H_0 of wCDM (see Fig. 6), compared to ΛCDM explains the minor shift to the left, while providing a solution to the Hubble tension. Remember that the cosmological parameter $\Omega_{k,0}$ for the spatial curvature has an analogous impact onto the spectrum. The degeneracy in the effect onto the spectrum between a change of spatial curvature and dark energy are well known, see e.g. Hu & Dodelson (2002).

In Sec. 3.1, we argue that the free-falling, comoving FLRW observer resides in a local inertial system, where SR applies and therefore perceives flat space. In the concept of the FLRW metric, the FLRW observer moves with freely streaming particles, which represent the galaxies in the Universe. The observations of the CMB in space missions have determined, along with the flatness of space, the temperature fluctuations in the CMB with an accuracy of the order of 10^{-5} K around the average background temperature of roughly 2.7 K. The expansion of the temperature power spectrum into spherical harmonics to display these measurements results do not include the first multipole moment, the dipole, for practical purposes. The dipole moment is induced by our peculiar motion against the CMB, and it is subtracted from the CMB raw data, because its amplitude of the order of 10^{-3} K would strongly dominate the other signal of interest. However, the fact that this dipole moment is still small, compared to the mean, just confirms that we – as observers here – fulfill the criterion of being comoving FLRW observers, not strictly (Peacock (1999)), but to a very high degree (a well-known fact, but see also e.g., von Hausegger (2024)). Indeed, this observational finding of a small dipole actually confirms that we comove with the expansion to a high degree. So, the metric we perceive is very close to the flat Minkowski metric.

The dipole, which corresponds to our peculiar motion against the CMB, however, offsets us from the perfectly comoving FLRW observer, who observes a perfectly flat space. Consequently, we now expand the scope and take into account our peculiar motion relative to the CMB, caused by our "local" cosmological environment (see e.g., Tully et al. (2014)), considering the spatial curvature Ω_k (since $\Omega_k = 0$ only applies to the perfectly comoving FLRW observer). As is customary, we call the resulting model owCDM model[15]. The results are depicted in Fig. 8. Now, the deviation from the ΛCDM spectrum amounts to a ≲ 0.01% level (disregarding the higher deviations at small l,

---

[15]This acronym is customarily used for extensions to ΛCDM, when $w(z)$ is different from −1 and additionally a spatial curvature is applied; see, for example, Particle Data Group Review Chapter 28 Dark Energy Particle Data Group et al. (2022).

where the error bars in the actual CMB measurements are larger anyway).

Fig. 8. The CMB temperature power spectrum in ΛCDM (blue) and in our owCDM model (magenta). The relative differences are shown at the bottom of the panel, and amount to ∼ 0.01%.

We find a spatial curvature of $\Omega_{k,0} = -0.0197$ that describes a local effect, induced by our "local" attractive cosmic environment, decoupling us from perfect Hubble flow (see Tully et al. (2014)). This value is compatible with the final PR4 of the Planck mission (Tristram et al. (2024)) with $\Omega_{k,0} = -0.012 \pm 0.010$.

In addition, we find for the owCDM model $S_8 = 0.798$, which is within 1σ with DES-Y3's result of $S_8 = 0.782 \pm 0.019$. Upon our fitting, we can improve our equation (30) which describes the evolution of w_{de}, according to

$$w_{de}(a) = \begin{cases} w_{de,early} & \text{when } a \le 1/6 \\ w_{de,early} + \left[\frac{(1/a-1)-5}{5}\right](w_{de,early} + 0.91) \\ \qquad \text{when } a > 1/6. \end{cases} \tag{31}$$

To reiterate, we stress that the evolution of w_{de} with cosmic time and the spatial curvature $\Omega_{k,0} = -0.0197$ are both effects of the nonlinear structure formation. The time-dependence of w_{de} is a global effect by the voids dominating the volume of the Universe, whereas $\Omega_{k,0} = -0.0197$ is a local effect by our local attractive cosmic environment, decoupling us from perfect Hubble flow.

8. Summary

We proposed two extensions to ΛCDM, wCDM and owCDM, which include the following novelties, on which we comment in the course of this section: a) We take the equivalence principle and the concept of the comoving FLRW observer at face value and find that the geometry of the Universe as given by the FLRW metric and the curvature of space are two individual quantities, where we identify the geometry with the DE component of our proposed extensions to ΛCDM. b) In the FLRW formalism, the density parameters of subcritical and supercritical universes are also normalized to critical density by considering the suitable amount of spatial curvature. In contrast to this, we consider the consequence of the equivalence principle that irrespective of the geometry (open, closed or flat) of a universe, observers in the

reference frame of the comoving FLRW observer, always perceive flat space. Thus, comoving (i.e., free-falling) observers in subcritical, supercritical or universes at critical density likewise perceive spatial flatness. c) The FLRW formalism and therefore also ΛCDM consider the energy densities in the early Universe as the initial conditions determining the expansion history of the Universe. In contrast, we consider these initial energy densities in relation to the post big bang expansion rate as the initial conditions. The relation between these two quantities determines the geometry of the Universe as described by the curvature of the FLRW metric. d) Customarily, the averaging problem only considers the density of (linear and non-linear) perturbations and finds that there is no significant backreaction onto the evolution of the background universe. We additionally consider the volume of perturbations and find a mild backreaction, caused by voids dominating the volume of the Universe, providing a possible solution to the Hubble tension problem. e) In owCDM we include the effect of the CMB dipole, which is otherwise not included in the calculations of FLRW models. This provides an explanation for the curvature of space measured by PR4 of the Planck mission (Tristram et al. (2024)) as the mere effect of our peculiar motion against the CMB, which "decouples" us from the Hubble flow.

We argued in Sec. 3.1 that the observation of flat space does not necessarily imply that we live in a universe with global flat space, expressed by zero curvature in the Einstein equations. In fact, an observation of flat space, as perceived by the comoving FLRW observer in the local inertial system, on the grounds of the equivalence principle, should apply likewise to flat, open and closed geometries of the FLRW metric. In Sec. 3.2, we exemplified that the initial conditions in the early Universe are given by the initial energy densities *and* the initial expansion rate obtained from the big bang.

In order to account for arbitrary expansion rates obtained from the big bang, not just the fine-tuned case of ΛCDM, in Sec. 4 we incorporate the initial expansion rate into the ΛCDM formalism. We identify the geometry of the Universe induced by the FLRW metric and the curvature term in the Friedmann equation (5), respectively, with ρ_{de} and express the perceived spatial flatness by $\rho_k = 0$. We associated an EoS with ρ_{de}, which depends on the amount of the energy content in the Universe (different from the operationally defined usual quantities ρ_{de} and ρ_k). Thus, ρ_{de} (along with w_{de}) describes the dynamics of the expansion of the background universe, as determined by the ICs of the Universe, and is not a "physical substance," in contrast to the assumption of the cosmological constant Λ. Nevertheless, we use the fluid formalism to include its impact into the energy momentum tensor $T_{\mu\nu}$, just in the same way it is done in ΛCDM. The wCDM model explains the phenomenology of a late-time accelerated expansion as a kinematic effect, induced by the primeval expansion rate H_{ini} in relation to the initial density, originating from the big bang. By choosing the same present-day matter content of $\Omega_{m,0} \simeq 0.3$ as in ΛCDM, we find $w_{de} \simeq -0.8$, very close to −1 of a cosmological constant. To reiterate, the Universe is, according to the wCDM model, described as subcritical Universe. This is different to ΛCDM, where the cosmological constant Λ is thought of as a kind of "physical substance" just like matter or radiation, as part of the energy-momentum tensor, which renders the Universe to be at critical density.

In the subsequent Sec. 5, we reconsidered the impact of the nonlinear structure formation in the late epochs of the Universe, especially in the form of its cosmic web, once voids domi-

nate the Universe in volume and (under-)density. We incorporated the impact of backreaction from cosmic voids onto the expansion history by way of its effect onto the EoS parameter w_{de}. As a result, the initially constant w_{de} morphs into a time-dependent function. We derived this function, using void models informed by cosmological ΛCDM simulations of the previous literature. This is justified, since we adopt the same standard CDM paradigm in our ΛCDM extensions (wCDM and owCDM). In Sec. 6, we compared the results from computations of ΛCDM and wCDM. The initially constant EoS parameter, $w_{de} \simeq -0.8$, evolves to a more negative value of $w_{de} \simeq -0.9$ at the present time, once the impact by voids has become significant. While this impact by voids onto the expansion history affects an overall change of only about 8% in the expansion rate of the late Universe, it is enough in order for our wCDM model to explain the Hubble tension problem, which refers to the offset between measurements of the Hubble constant H_0, using the CMB versus standard candles in the "local" Universe. We implemented wCDM into our amended version of the open-source Boltzmann code CLASS, in order to calculate the expansion history and the linear power spectra of this model. We compared our results with concordance ΛCDM, as well as with observations, and found that wCDM agrees well with current data, such as the Dark Energy Survey.

Owing to the different evolution of ρ_{de} in our ΛCDM extension versus Λ in ΛCDM, there is a difference in the age of the models, namely 13.04 Gyr versus 13.8 Gyr, respectively. We checked to see that the younger age of wCDM is not in conflict with age estimates of the oldest known stars. It is also not in conflict with the very early galaxies found by the James Webb Space Telescope, since the redshift determinations of these galaxies require a cosmological model to convert redshift into age. In a wCDM universe, these galaxies would be correspondingly younger than in a ΛCDM universe.

Furthermore, there are indications from observations that the evolution of the expansion rate H at low redshift is in conflict with the assumption of a cosmological constant, and dynamical models of DE with a time-dependent EoS parameter may be preferred; see for example Dainotti et al. (2022b, 2021, 2022a); Bargiacchi et al. (2023b,a); Ó Colgáin et al. (2021) and Krishnan et al. (2021). These results may indicate that the origin of the Hubble tension is likely to be in cosmology and not in local measurement issues, which we discuss in detail in Foidl & Rindler-Daller (2024). Also, in that paper we find that the Hubble tension problem can be explained phenomenologically in a very natural way by a DE component with a decreasing EoS parameter $w(z)$. Our ΛCDM extension described in this paper fulfills this property.

In the asymptotic future, the EoS parameter w_{de} converges to the one of a cosmological constant with a value of −1 (see Fig. 4). In fact, the future point in time where the effective EoS parameter (including all cosmic components) is very close to this value of −1 is not much different between wCDM and concordance ΛCDM.

In the final step, we compared the CMB temperature spectra of wCDM and ΛCDM. We find that wCDM's spectrum is shifted slightly to the left-hand side, while the amplitudes and structure of the peaks match perfectly. We explain this shift as the effect due to the increase of the expansion rate in our model, compared to ΛCDM. Subsequently, we fitted wCDM to ΛCDM's CMB temperature spectrum, as well as to the locally measured

value of $H_0 = 73.04$ by Riess et al. (2022), while we additionally considered spatial curvature. The resulting owCDM model reproduces ΛCDM's CMB spectrum at a 0.01% level, where the model parameters additionally include $\Omega_{k,0} = -0.0197$, which is very well compatible with the final PR4 of the Planck mission (Tristram et al. (2024)). We explain the spatial curvature as an effect of our "local" attractive cosmological environment (see e.g. Tully et al. (2014)), which offsets us from the position of a perfectly comoving FLRW observer, described by $\Omega_{k,0} = 0$, thus decoupling us from the Hubble flow, seen as a dipole in the CMB measurements. This dipole does not enter the computations in ΛCDM, though. In addition to providing a solution to the Hubble tension, we find that both, wCDM and owCDM, also mitigate the σ_8 tension.

In conclusion, we like to note that we presented two extensions to ΛCDM, which are based on a time-dependent evolution of the EoS parameter $w(z)$ of the "DE component". In contrast to other parameterisations, like the empirically defined CPL parameterisation, we conceived our DE model based on well-accepted concepts and theories, already applied in ΛCDM. Furthermore, our extensions wCDM and owCDM can be tested, using ongoing and future observational campaigns, within their current scope. Only minor adaptation to the process of data analysis is required to implement our extensions into these campaigns, as we also exemplify in Foidl & Rindler-Daller (2024), and where we present a list of observational programs of interest. By determining the EoS of DE, these programs will be able to rule out our extensions or confirm them by providing an even more accurate update of our function of $w_{\mathrm{de}}(z)$, i.e. a more observationally informed EoS, compared to our approximations, based on the Millennium simulation, in this paper.

References

Abbott, T. M. C., Aguena, M., Alarcon, A., et al. 2022, Phys. Rev. D, 105, 023520

Abbott, T. M. C., Aguena, M., Alarcon, A., et al. 2023, Phys. Rev. D, 107, 083504

Amendola, L. & Tsujikawa, S. 2010, Dark Energy (Cambridge University Press)

Barausse, E., Matarrese, S., & Riotto, A. 2005, Phys. Rev. D, 71, 063537

Bargiacchi, G., Dainotti, M. G., & Capozziello, S. 2023a, MNRAS, 525, 3104

Bargiacchi, G., Dainotti, M. G., Nagataki, S., & Capozziello, S. 2023b, MNRAS, 521, 3909

Birkhoff, G. D. & Langer, R. E. 1923, Relativity and modern physics (Harvard University Press)

Bondi, H. 1947, MNRAS, 107, 410

Buchert, T. 2000, General Relativity and Gravitation, 32, 105

Buchert, T. 2001, General Relativity and Gravitation, 33, 1381

Buchert, T. 2011, Classical and Quantum Gravity, 28, 164007

Buchert, T., Carfora, M., Ellis, G. F. R., et al. 2015, Classical and Quantum Gravity, 32, 215021

Buchert, T. & Ehlers, J. 1997, A&A, 320, 1

Calzetta, E. A., Hu, B. L., & Mazzitelli, F. D. 2001, Phys. Rep., 352, 459

Camarena, D. & Marra, V. 2020, Physical Review Research, 2, 013028

Carloni, S., Leach, J. A., Capozziello, S., & Dunsby, P. K. S. 2008, Classical and Quantum Gravity, 25, 035008

Cautun, M., van de Weygaert, R., Jones, B. J. T., & Frenk, C. S. 2014, MNRAS, 441, 2923

Chevallier, M. & Polarski, D. 2001, International Journal of Modern Physics D, 10, 213

Cimatti, A. & Moresco, M. 2023, ApJ, 953, 149

Colberg, J. M., Sheth, R. K., Diaferio, A., Gao, L., & Yoshida, N. 2005, MNRAS, 360, 216

Coles, P. & Lucchin, F. 2002, Cosmology: The Origin and Evolution of Cosmic Structure, Second Edition (Wiley-VCH, July)

Correnti, M., Gennaro, M., Kalirai, J. S., Cohen, R. E., & Brown, T. M. 2018, ApJ, 864, 147

Curtis-Lake, E., Carniani, S., Cameron, A., et al. 2023, Nature Astronomy, 7, 622

Dainotti, M. G., Bargiacchi, G., Bogdan, M., Capozziello, S., & Nagataki, S. 2023, arXiv e-prints, arXiv:2303.06974

Dainotti, M. G., De Simone, B., Schiavone, T., et al. 2021, ApJ, 912, 150

Dainotti, M. G., De Simone, B. D., Schiavone, T., et al. 2022a, Galaxies, 10, 24

Dainotti, M. G., Nielson, V., Sarracino, G., et al. 2022b, MNRAS, 514, 1828

de Bernardis, P., Ade, P. A. R., Bock, J. J., et al. 2000, Nature, 404, 955

de Sitter, W. 1917, Koninklijke Nederlandse Akademie van Wetenschappen Proceedings Series B Physical Sciences, 19, 1217

Di Valentino, E., Mena, O., Pan, S., et al. 2021, Classical and Quantum Gravity, 38, 153001

Dodelson, S. 2003, Modern cosmology (Academic Press)

Ellis, G. F. R. 1983, in General Relativity and Gravitation, Volume 1, ed. B. Bertotti, F. de Felice, & A. Pascolini, Vol. 1, 668

Finkelstein, S. L., Bagley, M. B., Ferguson, H. C., et al. 2023, ApJ, 946, L13

Flanagan, É. É. 2005, Phys. Rev. D, 71, 103521

Fließbach, T. 2016, Allgemeine Relativitätstheorie

Foidl, H. & Rindler-Daller, T. 2024, A&A, 686, A210

Friedmann, A. 1922, Zeitschrift fur Physik, 10, 377

Friedmann, A. 1924, Zeitschrift fur Physik, 21, 326

Gasperini, M., Marozzi, G., & Veneziano, G. 2009, J. Cosmology Astropart. Phys., 2009, 011

Geshnizjani, G., Chung, D. J., & Afshordi, N. 2005, Phys. Rev. D, 72, 023517

Grebel, E. K. 2012, in American Institute of Physics Conference Series, Vol. 1480, First Stars IV - from Hayashi to the Future -, ed. M. Umemura & K. Omukai, 172–183

Grebel, E. K. 2016, in Star Clusters and Black Holes in Galaxies across Cosmic Time, ed. Y. Meiron, S. Li, F. K. Liu, & R. Spurzem, Vol. 312, 157–170

Gruzinov, A., Kleban, M., Porrati, M., & Redi, M. 2006, J. Cosmology Astropart. Phys., 2006, 001

Guth, A. H. 1981, Phys. Rev. D, 23, 347

Harrison, E. R. 2000, Cosmology. The science of the universe. (Cambridge University Press)

Hinshaw, G., Larson, D., Komatsu, E., et al. 2013, ApJS, 208, 19

Hirata, C. M. & Seljak, U. 2005, Phys. Rev. D, 72, 083501

Hogg, D. W., Eisenstein, D. J., Blanton, M. R., et al. 2005, ApJ, 624, 54

Hu, W. & Dodelson, S. 2002, ARA&A, 40, 171

Icke, V. 1984, MNRAS, 206, 1P

Icke, V. 2001, in Astronomical Society of the Pacific Conference Series, Vol. 252, Historical Development of Modern Cosmology, ed. V. J. Martínez, V. Trimble, & M. J. Pons-Bordería, 337

Icke, V. & van de Weygaert, R. 1987, A&A, 184, 16

Icke, V. & van de Weygaert, R. 1991, QJRAS, 32, 85

Jebsen, J. T. 1921, Arkiv for Matematik, Astronomi och Fysik, 15, 18

Jebsen, J. T. 2005, General Relativity and Gravitation, 37, 2253

Kamionkowski, M. & Riess, A. G. 2023, Annual Review of Nuclear and Particle Science, 73, 153

Khalife, A. R., Zanjani, M. B., Galli, S., et al. 2024, J. Cosmology Astropart. Phys., 2024, 059

Kolb, E. W., Matarrese, S., Notari, A., & Riotto, A. 2005, Phys. Rev. D, 71, 023524

Kolb, E. W. & Turner, M. S. 1990, The early universe, Vol. 69 (CRC Press)

Krishnan, C., Ó Colgáin, E., Sheikh-Jabbari, M. M., & Yang, T. 2021, Phys. Rev. D, 103, 103509

Kumar, N. & Flanagan, É. É. 2008, Phys. Rev. D, 78, 063537

Kwan, J., Francis, M. J., & Lewis, G. F. 2009, MNRAS, 399, L6

Lemaître, G. 1927, Annales de la Société Scientifique de Bruxelles, 47, 49

Lemaître, G. 1933, Annales de la Société Scientifique de Bruxelles, 53, 51

Lemaître, G. A. & MacCallum, M. A. H. 1997, General Relativity and Gravitation, 29, 641

Lesgourgues, J. 2011, arXiv e-prints, arXiv:1104.2932

Li, N. & Schwarz, D. J. 2007, Phys. Rev. D, 76, 083011

Linder, E. V. 2003, Phys. Rev. Lett., 90, 091301

Ma, C.-P. & Bertschinger, E. 1995, ApJ, 455, 7

Maciel, A., Le Delliou, M., & Mimoso, J. P. 2018, Phys. Rev. D, 98, 024016

MacTavish, C. J., Ade, P. A. R., Bock, J. J., et al. 2006, ApJ, 647, 799

Martineau, P. & Brandenberger, R. 2005, arXiv e-prints, astro

Milne, E. A. 1933, ZAp, 6, 1

Mukhanov, V. 2005, Physical Foundations of Cosmology (Cambridge University Press)

Notari, A. 2006, Modern Physics Letters A, 21, 2997

Ó Colgáin, E., Sheikh-Jabbari, M. M., & Yin, L. 2021, Phys. Rev. D, 104, 023510

Okabe, A., Boots, B., & Sugihara, K. 2000, Spatial tessellations. Concepts and Applications of Voronoi diagrams (John Wiley)

Paranjape, A. 2009, PhD thesis, Tata Institute of Fundamental Research, Mumbai, India

Parry, M. 2006, J. Cosmology Astropart. Phys., 2006, 016

Particle Data Group, P. D. G., Workman, R. L., Burkert, V. D., et al. 2022, Progress of Theoretical and Experimental Physics, 2022, 083C01

Peacock, J. A. 1999, Cosmological Physics (Cambridge University Press)

Peebles, P. J. E. 1993, Principles of Physical Cosmology (Princeton University Press)

Perlmutter, S. 2003, Physics Today, 56, 53

Perlmutter, S., Aldering, G., Goldhaber, G., et al. 1999, ApJ, 517, 565

Planck-Collaboration. 2020, A&A, 641, A1

Poulin, V., Smith, T. L., & Karwal, T. 2023, Physics of the Dark Universe, 42, 101348

Rácz, G., Dobos, L., Beck, R., Szapudi, I., & Csabai, I. 2017, MNRAS, 469, L1

Räsänen, S. 2006a, J. Cosmology Astropart. Phys., 2006, 003

Räsänen, S. 2006b, Classical and Quantum Gravity, 23, 1823

Rebouças, J., Gordon, J., de Souza, D. H. F., et al. 2024, J. Cosmology Astropart. Phys., 2024, 042

Ricciardelli, E., Quilis, V., & Planelles, S. 2013, MNRAS, 434, 1192

Riess, A. G., Filippenko, A. V., Challis, P., et al. 1998, AJ, 116, 1009

Riess, A. G., Yuan, W., Macri, L. M., et al. 2022, ApJ, 934, L7

Robertson, B. E., Tacchella, S., Johnson, B. D., et al. 2023, Nature Astronomy, 7, 611

Robertson, H. P. 1935, ApJ, 82, 284

Robertson, H. P. 1936a, ApJ, 83, 187

Robertson, H. P. 1936b, ApJ, 83, 257

Schmidt, B. P., Suntzeff, N. B., Phillips, M. M., et al. 1998, ApJ, 507, 46

Scrimgeour, M. I., Davis, T., Blake, C., et al. 2012, MNRAS, 425, 116

Shandarin, S., Feldman, H. A., Heitmann, K., & Habib, S. 2006, MNRAS, 367, 1629

Siegel, E. R. & Fry, J. N. 2005, ApJ, 628, L1

Smoot, G. F., Bennett, C. L., Kogut, A., et al. 1992, ApJ, 396, L1

Springel, V., White, S. D. M., Jenkins, A., et al. 2005, Nature, 435, 629

Steigman, G. 2007, Annual Review of Nuclear and Particle Science, 57, 463

Stoeger, W. R., Helmi, A., & Torres, D. F. 2007, International Journal of Modern Physics D, 16, 1001

Tolman, R. C. 1934, Proceedings of the National Academy of Science, 20, 169

Tristram, M., Banday, A. J., Douspis, M., et al. 2024, A&A, 682, A37

Tully, R. B., Courtois, H., Hoffman, Y., & Pomarède, D. 2014, Nature, 513, 71

Van Acoleyen, K. 2008, J. Cosmology Astropart. Phys., 2008, 028

van de Weygaert, R. 1994, A&A, 283, 361

van de Weygaert, R. & Icke, V. 1989, A&A, 213, 1

von Hausegger, S. 2024, MNRAS, 535, L49

Voronoi, G. 1908, Journal für die reine und angewandte Mathematik, 134, 198

Walker, A. G. 1937, Proceedings of the London Mathematical Society, 42, 90

Weinberg, S. 1972, Gravitation and Cosmology: Principles and Applications of the General Theory of Relativity

Weinberg, S. 2008, Cosmology (Oxford University Press, Oxford, UK)

Wetterich, C. 2003, Phys. Rev. D, 67, 043513

Wiltshire, D. L. 2007, New Journal of Physics, 9, 377

Wiltshire, D. L. 2011, Classical and Quantum Gravity, 28, 164006